COPY 1

Report No. FAA-RD-74-88, II

ANA-64

ASR-5 RADAR
DUAL FEEDHORN ANTENNA MODIFICATION

VOLUME II - DESCRIPTION OF FEASIBILITY EFFORT

P.E. RAWLINSON

April 1974

Final Report

Document is available to the public through the
National Technical Information Service,
Springfield, Virginia 22151

Prepared for

U.S. DEPARTMENT OF TRANSPORTATION

FEDERAL AVIATION ADMINISTRATION

Systems Research & Development Service

Washington, D.C. 20590

TECHNICAL REPORT STANDARD TITLE PAGE

1. Report No.	2. Government Accession No.	3. Recipient's Catalog No.
FAA-RD-74-88, II		

4. Title and Subtitle	5. Report Date
ASR-5 Radar Dual Feedhorn Antenna Modification Volume II -Description of Feasibility Effort	April 1974
	6. Performing Organization Code
7. Author(s) P. E. Rawlinson	8. Performing Organization Report No.
9. Performing Organization Name and Address Raytheon Company Equipment Division Wayland Laboratory Wayland, Mass.	10. Work Unit No.
	11. Contract or Grant No. DOT-FA69WA-2129
12. Sponsoring Agency Name and Address Department of Transportation Federal Aviation Administration Systems Research and Development Service Washington, D. C. 20590	13. Type of Report and Period Covered Final Report June 1969 - August 1972
	14. Sponsoring Agency Code

15. Supplementary Notes

This report is issued in two volumes. Volume I contains the description of hardware and summary of feasibility effort. Volume II contains the description of feasibility effort.

16. Abstract

The objective of this program is to produce separate antenna two-way coverage patterns for the close-in and long range capabilities of the terminal radar system. The feedhorn geometry of the ASR-5 antenna was modified by adding a separate receive only feedhorn and polarizer. The close-in coverage was obtained by transmission on the normal (low) beam and reception on the second (high or tilted-up) beam. The long range coverage was obtained by both transmission and reception on the normal beam.

This program was divided into two phases. Phase I involves the work performed to determine the feasibility of a dual feedhorn configuration to be employed with an ASR-5 antenna. Phase II concerns the design and test of the hardware to be delivered to the FAA for evaluation with an ASR-5.

The results and conclusions drawn from this program were that the receive-only antenna pattern had an acceptable sidelobe level, azimuth beamwidth, elevation beam shape, and integrated cancellation ratio; that the normal ASR-5 antenna pattern suffered minimal degradation inboth linear and circular polarization; and that a field modification of this system is feasible.

17. Key Words :	18. Distribution Statement :
Airport Surveillance Radar, Dual Feedhorn Antenna, Passive Horn, Air Traffic Control, Ground Clutter, Angel Clutter, Radar Antenna	Document is available to the public through the National Technical Information Service, Springfield, Virginia 22151

19. Security Classif. (of this report)	20. Security Classif. (of this page)	21. No. of Pages	22. Price
UNCLASSIFIED	UNCLASSIFIED	118	

Form DOT F 1700.7 (8-69)

TABLE OF CONTENTS

	Page
INTRODUCTION	1
ENGINEERING ANALYSES	3
Antenna Geometry	3
Computations	3
Elevation Plane Patterns	3
ICR Values	13
ANTENNA DESIGN	16
Feedhorns	16
Radome	19
Second Feedhorn Orthogonal Inputs	19
Second Feedhorn Polarizer Switch	27
RF-Combining Network	27
EXPERIMENTAL MEASUREMENTS	38
Test Range	38
Test Set-Up	38
Test Procedure	44
Pattern Data	47
Test Data Evaluation	47
COVERAGE CONSIDERATIONS	108
CONCLUSIONS	115
REFERENCES	116

INTRODUCTION

This Phase I Final Report discusses the efforts carried out to determine the feasibility of a dual feedhorn configuration to be employed with the doubly-curved ASR-5 antenna reflector. The feedhorn geometry is modified to provide a tilted up, receive only, second elevation plane pattern in addition to the normal elevation plane pattern of the original design.

The intent of this terminal radar antenna modification program is to produce separate antenna two-way coverage patterns for the close-in and long-range capabilities of the radar system. It is intended that the close-in coverage will be obtained by transmission on the normal (low) beam and reception on the second (high) beam. The long-range coverage will be obtained by both transmission and reception on the normal beam. It is expected that the antenna will be tilted down one or more degrees from the typical unmodified ASR-5 design elevation angle.

For the purposes of the Phase I effort it was most important that the angular separation of the normal and second elevation plane patterns be altered to satisfy three different conditions. The three separation conditions are specifically defined by considering the elevation angle of the lower (underside) half-power point of the normal beam elevation plane pattern and then causing the second beam elevation plane patterns at this angle to have one-way power strengths of 12, 16, and 20 dB down, respectively, from the normal beam pattern.

Previous work by Raytheon[1] showed that beam separations such as these were readily obtained (for a linearly polarized mode of operation in an ARSR-2 scale model antenna geometry) by combining at RF a small portion of the normal beam signal with a strong second beam signal to obtain the second (tilted-up) pattern. This same (RF-combining) approach is basic to the Phase I effort discussed herein. It will be shown below that this approach has successfully produced second beam patterns at the three specified separation conditions for both linear and circular polarization modes of operation. Full frequency bandwidth performance has also been shown to be practical.

Other antenna pattern parameters considered in the effort are; (1) the second pattern gain objective is to be within 1 dB of the normal pattern gain, (2) azimuth plane sidelobes and beamwidths for the second pattern should be similar to those of the unmodified ASR-5 antenna, and (3) minimum degradation of the normal pattern for both linear and circular polarization should occur as a result of the modification. Although the gain objective could not be met with the ASR-5 antenna reflector, the remaining pattern parameters for the normal and second beams have proven to be satisfactory.

ENGINEERING ANALYSES

Antenna Geometry. - The central section curve coordinates for the ASR-5 antenna system were obtained from the drawings of the antenna of the similar AN/FPN-47 radar. From these coordinates, listed in Table 1, position of the design focal point for the ASR-5 reflector can be determined to be located as shown in Figure 1.

Furthermore, outgoing reflected ray planes at each central section point as determined by projecting outboard section points onto the central section plane[3] are in agreement with Dunbar's technique. It was somewhat surprising, however, to observe that the reflected rays associated with the lower one-fifth of the reflector pass through the focal point region as shown in Figure 2. This situation is often avoided in order to minimize any aperture blockage problems due to the feedhorn and its support platform.

Hopefully, when a second feed is positioned below the original feedhorn to generate a tilted up beam, somewhat less of the lower portion of the reflector will contribute toward aperture blockage for the second beam pattern since the outgoing rays at each central section point will be reflected at slightly higher elevation angles. It can be anticipated that considerable azimuth plane defocussing may be observed, however, for second source points that are located as much as six inches from the design focal point.

Computations. - Elevation Plane Patterns. - Approximating expressions for the secondary (far-field) elevation plane power pattern of a multiple point-source fed, shaped-beam, reflector antenna were devised and programmed to compute the power pattern in terms of the real and imaginary parts of the voltage pattern.

$$P(\phi) = [R(\phi)]^2 + [I(\phi)]^2$$

When the real and imaginary components are examined in detail for cases involving single sources and for cases involving multiple sources, considerable insight is provided into the possible pattern rippling (or even total cancellation) that could result from RF-combining of the shaped patterns associated with each individual source.

The real, $R(\phi)$, and imaginary, $I(\phi)$, parts of computed secondary elevation plane patterns for a source located at the (normal) design focal point (72, 0) and for a second (independent) source located slightly below (71.490, -4.855) the focal point are listed in Table II. These source points subtend a physical angle of four degrees from the reflector's mid-point.

Figure 3 is a voltage plot in the complex RI-plane for the computed normal feed pattern. Distributed along the curve are values of the elevation angle, ϕ. The maximum vector length occurs for an elevation angle of approximately 4.5° and represents the peak of the computed power pattern.

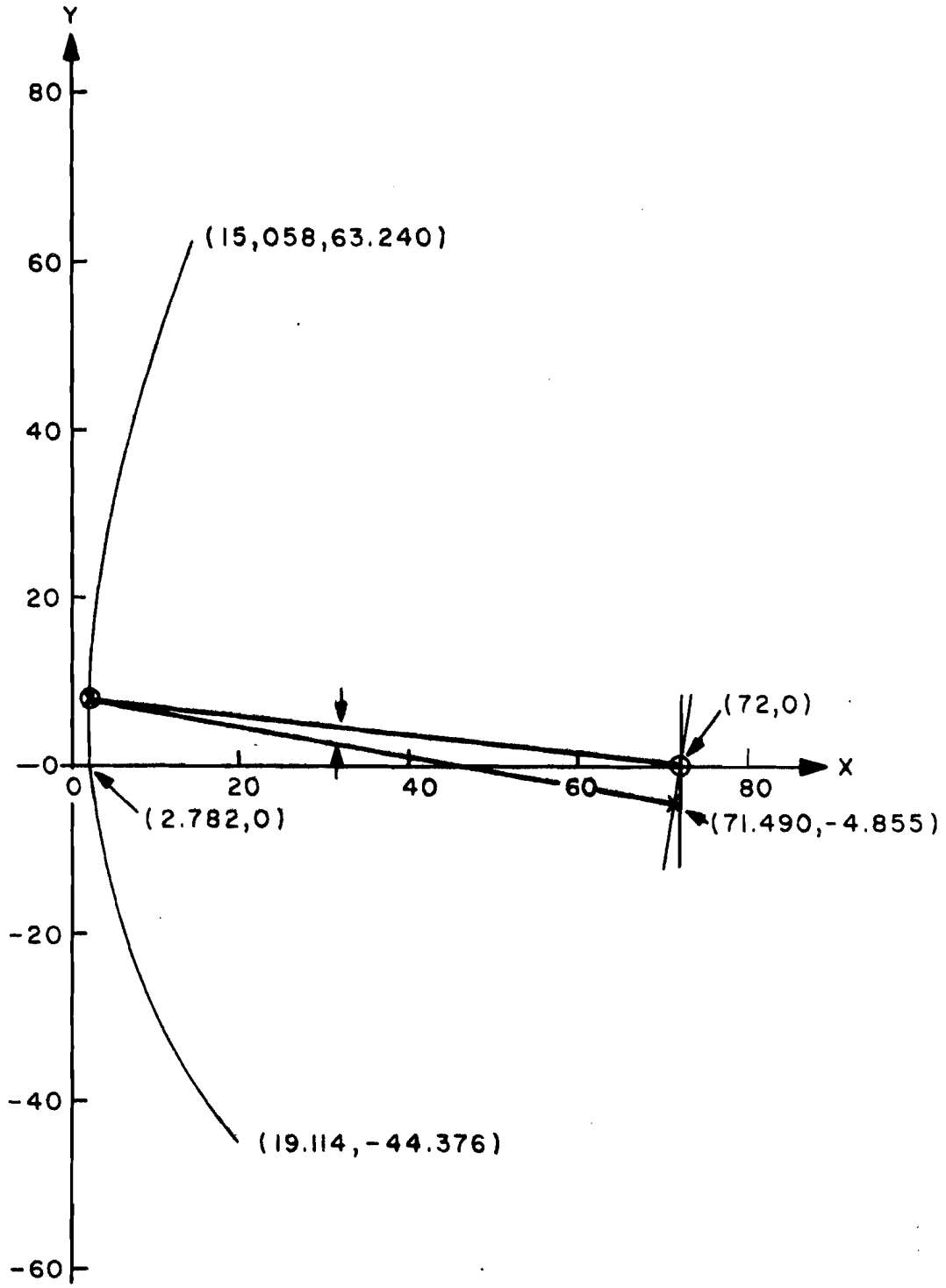

Figure 1. Reflector Central Section Geometry

TABLE II. Computed Secondary Patterns

	Normal Feed		Second Feed	
ϕ	Real	Imaginary	Real	Imaginary
-4.0	-0.0404	+0.1923	-0.3025	0.2206
-3.5	-0.2146	0.4115	-0.2515	0.1824
-3.0	-0.3920	0.3533	-0.0499	+0.0576
-3.5	-0.3870	+0.0015	+0.2331	-0.0518
-2.6	-0.0626	-0.4576	0.4523	-0.0667
-2.5	+0.5440	-0.7037	0.4617	+0.0071
-1.0	1.1748	-0.4508	0.2108	0.0766
-0.5	1.4324	+0.3712	-0.1989	+0.0262
0.0	+0.9629	1.5233	-0.5428	-0.1885
0.5	-0.3448	2.5157	-0.5862	-0.4788
1.0	-2.2530	2.8037	-0.2272	-0.6441
1.5	-4.2265	2.0310	+0.4132	-0.4763
2.0	-5.6294	+0.2023	1.0124	+0.1018
2.5	-5.9796	-2.3003	1.1846	0.9465
3.0	-5.1401	-4.8651	+0.6742	1.7098
3.5	-3.3612	-6.8902	-0.4919	1.9706
4.0	-1.1589	-8.0028	-1.9744	1.4242
4.5	+0.9053	-8.1631	-3.2359	+0.0372
5.0	2.4343	-7.6196	-3.7517	-1.9093
5.5	3.3062	-6.7572	-3.2205	-3.9148
6.0	3.6477	-5.9219	-1.6801	-5.4485
6.5	3.7071	-5.3054	+0.5189	-6.1464
7.0	3.7036	-4.9274	2.8605	-5.9286
7.5	3.7287	-4.7011	4.8595	-4.9925
8.0	3.7380	-4.5274	6.2187	-3.6966
8.5	3.6182	-4.3622	6.8883	-2.4011
9.0	3.2801	-4.2251	7.0187	-1.3401
9.5	2.7201	-4.1615	6.8497	-0.5762
10.0	+2.0234	-4.1901	6.5941	-0.0425
12.0	-0.2758	-4.0743	5.8318	+1.0965
14.0	-2.5148	-2.4024	4.8489	-0.5590
16.0	-3.3139	+0.2014	3.4997	-2.2799
18.0	-1.2005	2.9222	+0.9035	-3.7080
20.0	+1.7481	+1.9003	-2.0721	-2.8348
22.0	+2.5204	-0.9101	-3.2780	+0.4690
24.0	-0.9583	-2.7065	-0.8469	2.7135
26.0	-2.3535	+1.2134	+2.4010	+1.8442
28.0	+1.4979	+1.8046	+1.8932	-2.5955
30.0	+0.9190	-1.7904	-2.6052	-1.3294
32.0	-1.4938	+0.1444	-0.5807	+2.4785
34.0	+0.6458	+0.7418	+2.0517	-0.4157
36.0	+0.1926	-0.6329	-1.0096	-1.0621
38.0	-0.5091	+0.2894	-0.2469	+0.9228
40.0	+0.4403	-0.0709	+0.6815	-0.2617

The angular orientation of the vector represents the far-field phase of the pattern (here approximately $\eta = 280° + 360q$ at the pattern peak) relative to the positive real axis. Note that the far-field phase reverses direction near the power pattern's upper 3 dB point for the phase reference origin taken as in Figure 1.

Figure 4 is the similar voltage plot for the second (independent) feed pattern. The peak of this computed power pattern is found at an elevation angle of slightly less than 8.5° indicating that a beam deviation factor of nearly unity[4] probably exists for the ASR-5 reflector. For this pattern the far-field phase (here approximately $\sigma = 300° + 360q$ at the pattern peak) also reverses direction near the upper 3 dB point.

Figure 5 shows a voltage pattern when two sources are utilized; that is, RF-combining of the patterns of two point source feeds is invoked. The solid curve (the voltage pattern) has characteristics similar to the preceding figure for the second (independent) source. Examine the two vectors which contribute to the combined pattern vector $(\vec{S})$ at the 6° elevation angle. One vector (designated by

$$\sqrt{1-K_o^2}\ \vec{S}_{ind}\ )$$

is the slightly attenuated 6° - vector $(\vec{S}_{ind})$ of Figure 4 and the other vector (designated by $K_o\vec{N}$) is the greatly attenuated 6° - vector $(\vec{N})$ of Figure 3. A circle of radius K_oN and centered at the end point of the vector

$$\sqrt{1-K_o^2}\ \vec{S}_{ind}$$

is shown with four relative phase values indicated. The 0°-value has been taken consistent with the far-field phase value η of Figure 3 as the elevation angle is varied in the power pattern computation. It will be shown later that such circles represent the possible changes in the secondary pattern that will occur as the phasor, β, of the RF-combining network is varied. It will also be shown that the radial dimensions (i.e., K_o) of such circles nearly represent the possible changes in the secondary pattern when the amplitude control phasor, α, of the RF-combining network is varied.

It can be seen in Figure 5 that, for those elevation angles where the circles are tangent to the computed pattern curve (e.g., 7.5° and 20° in elevation), large excursions in the β-phase value (on either side of 0°) will produce a nearly constant magnitude resultant vector. Such points will appear as "stationary" points in the far-field power pattern associated with the RF-combining network phasor. For those elevation angles where the circles straddle the computed pattern curve (e.g., 6° in elevation), large excursions in the α-phase value (causing K_o to shrink through zero into negative values) will also produce a nearly constant magnitude resultant vector Such points will appear as "stationary" points in the far-field power pattern associated with the RF-combining network amplitude control phasor.

The same type of effects obviously would appear if the amount of signal attenuations were reversed. Figure 6 is a measured elevation plane pattern wherein the β-phase value is being varied and the α-phase value has been selected such that the normal feed pattern is only slightly attenuated through

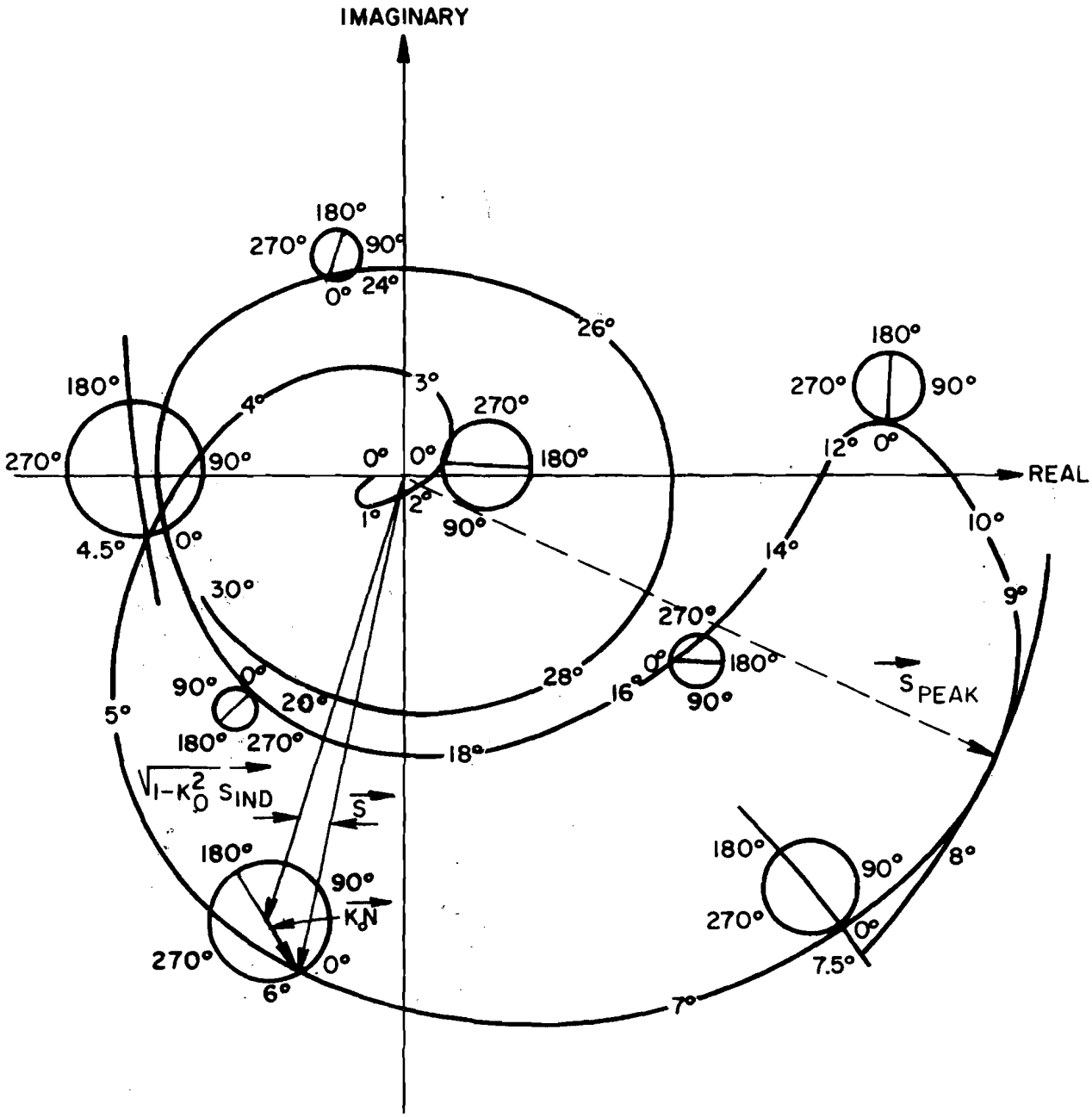

Figure 5. Computed RF-Combined Second Feed Pattern

the RF-combining network and the second (independent) feed pattern is greatly attenuated. Stationary points appear at 1°, 3.5°, 8°, 17°, and 26° in elevation. Examination at the lower (underside) 3 dB points of these measured pattern shapes emphasizes the insignificant one-way power strength variation that occurs for such α-phase settings. That is, it is evident that α-phase values which cause the second (independent) feed pattern to predominate are necessary to obtain the desired combined patterns.

ICR Values. - The computational procedure ordinarily utilized for calculating integrated cancellation ratios[5] (ICRs) implies the use of the same circularly polarized antenna for both transmission and reception. For a dual antenna system the ICR value calculation for a composite beam (N/S, i.e., transmission on the normal beam with reception on the second beam) is given by the equation

$$ICR_{dB} = 10 \log_{10} \frac{\Sigma_{\theta,\phi} (E_a^2 + E_b^2)\ (E_c^2 + E_d^2) \cos \phi}{\Sigma_{\theta,\phi}[(E_aE_c - E_bE_d)^2 \cos^2(\tau_1 - \tau_2) + (E_aE_d - E_bE_c)^2 \sin^2 (\tau_1 - \tau_2)]\cos \phi}$$

where

$E_a = {}_1P_{max}^{\frac{1}{2}}$ $\qquad$ $E_c = {}_2P_{max}^{\frac{1}{2}}$

$E_b = {}_1P_{min}^{\frac{1}{2}}$ $\qquad$ $E_d = {}_2P_{min}^{\frac{1}{2}}$

τ_1 = polarization tilt angle of beam 1

τ_2 = polarization tilt angle of beam 2

and

ϕ = elevation plane angle above horizon

Beam 1 is typically the normal feed pattern and beam 2 the second feed pattern for the composite case. It can be shown that, when the same pattern is used for transmission and reception (i.e., $E_a = E_c$, $E_b = E_d$, and $\tau_1 = \tau_2$), this equation reduces to the calculation given in the reference.

Table III shows the output format of the computer program devised to calculate ICR values for the measured circular polarization properties of the modified antenna. The first line of the output data indicates that pattern charts #49 and #50 from the measurement test procedure (being azimuth cuts at the +5° elevation angle with the reflector oriented in position V) contain the input data. The case is further identified as the computation for the frequency of 2.8 GHz and the 20 dB beam separation condition.

Five two-way ICR values are computed. The first two listed are for transmission and reception on the same pattern; first the normal (low) beam, and next the second (high) beam. The third value listed (25.69 dB) is for the important composite (N/S) beam case of transmission on the normal beam and reception on the second beam where the orientation angles of both

polarization patterns significantly influence the ICR value. The last two values listed show how the worst case ellipse orientation and the best case ellipse orientation might influence the situation (if one could successfully control this parameter over the total beam pattern at all frequencies).

The many ICR values computed during the Phase I effort are plotted in Figures 38 through 47 in the section entitled Test Data Evaluation.

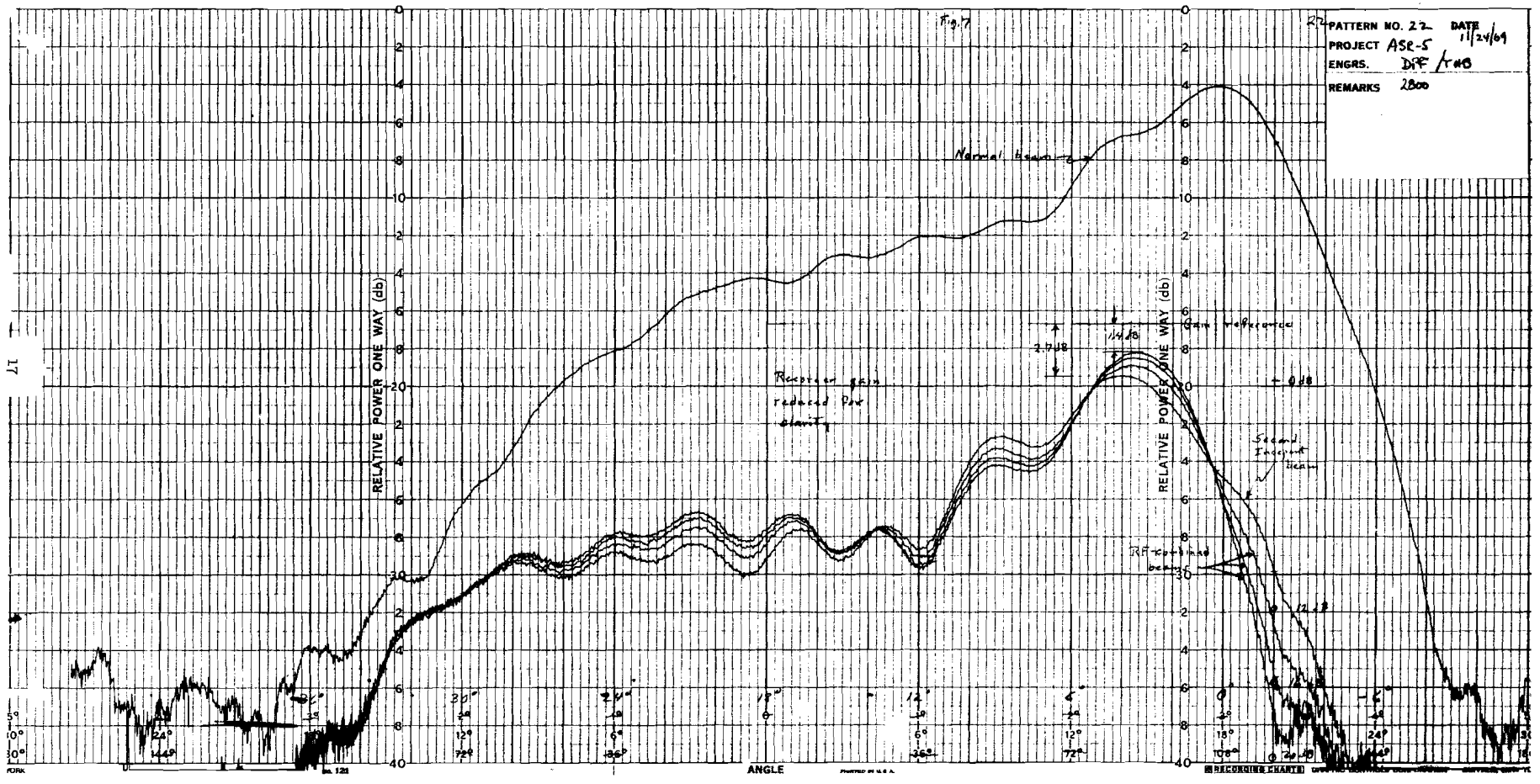

Figure 7. Measured Secondary Patterns for 2.6" Square Aperture Second Feedhorn

Figure 9 is a photograph of the dual-aperture feedhorn assembly for the 3.3" x 4.7" rectangular aperture second feedhorn case. Both feedhorn apertures are shown as coplanar here but other feed horn alignments were experimentally measured. Note further that a dummy normal feedhorn is being employed for the linearly polarized investigation of this particular set-up.

Figure 10 contains a set of measured elevation plane patterns with and without RF-combining for the rectangular aperture second feedhorn. Observe that the pattern peak value of the second feed without RF-combining (labelled "Second independent beam") is approximately 3.2 dB below the pattern peak of the normal feed. Again, the 1 dB gain objective is not achieved, although the upper angle elevation coverage is quite smooth for all second feed patterns.

Figure 11 is a photograph of the final feedhorn assembly without a radome in place. The second feedhorn aperture here has comparable internal ribs and external corner tabs to those of the original ASR-5 feedhorn aperture. This total breadboard assembly is believed to be readily adaptable into a field modification kit which would require minimum downtime for installation.

Radome. - The spherical-cap shape of the unmodified ASR-5 radome is not compatible with the extended vertical aperture of a dual feedhorn configuration. Thus the original radome was removed and replaced with a fiberglass cylindrically shaped radome. The first such radome fabricated was made to the same 0.125" thickness of the original radome. Secondary pattern measurements made with this radome in place indicated a severe squinting of the elevation pattern peak existed. Figure 12 is a measured comparison pattern and with this so-called thick radome in place. Several attempts to reduce the squint by varying the location of an internal flat sheet of fiberglass were unsuccessful. A thinner skinned radome was therefore fabricated.

The thin (0.032" in thickness) fiberglass radome shown in Figure 13 can be seen to be optically translucent. Figure 14 shows more clearly the cylindrical shape. TABLE IV lists ICR values for the normal beam patterns measured in the unmodified geometry and with the final modified dual-feedhorn geometry. No degradation in performance is found herein.

Second Feedhorn Orthogonal Inputs. Because the feed support boom of the unmodified ASR-5 antenna leaves little space beneath the normal feedhorn and its polarizer switch and because it seemed very desirable not to cut away (nor even cut into) the mechanical structure of the boom, a very short dual mode coax-to-waveguide transition was deemed necessary as the second feedhorn aperture size became larger. Figure 9 shows clearly the limited space available without significant rework of the boom endplate and the normal feedhorn's polarizer platform.

It is believed that the short breadboard transition successfully designed and utilized herein might be improved slightly during the proposed Phase II effort.

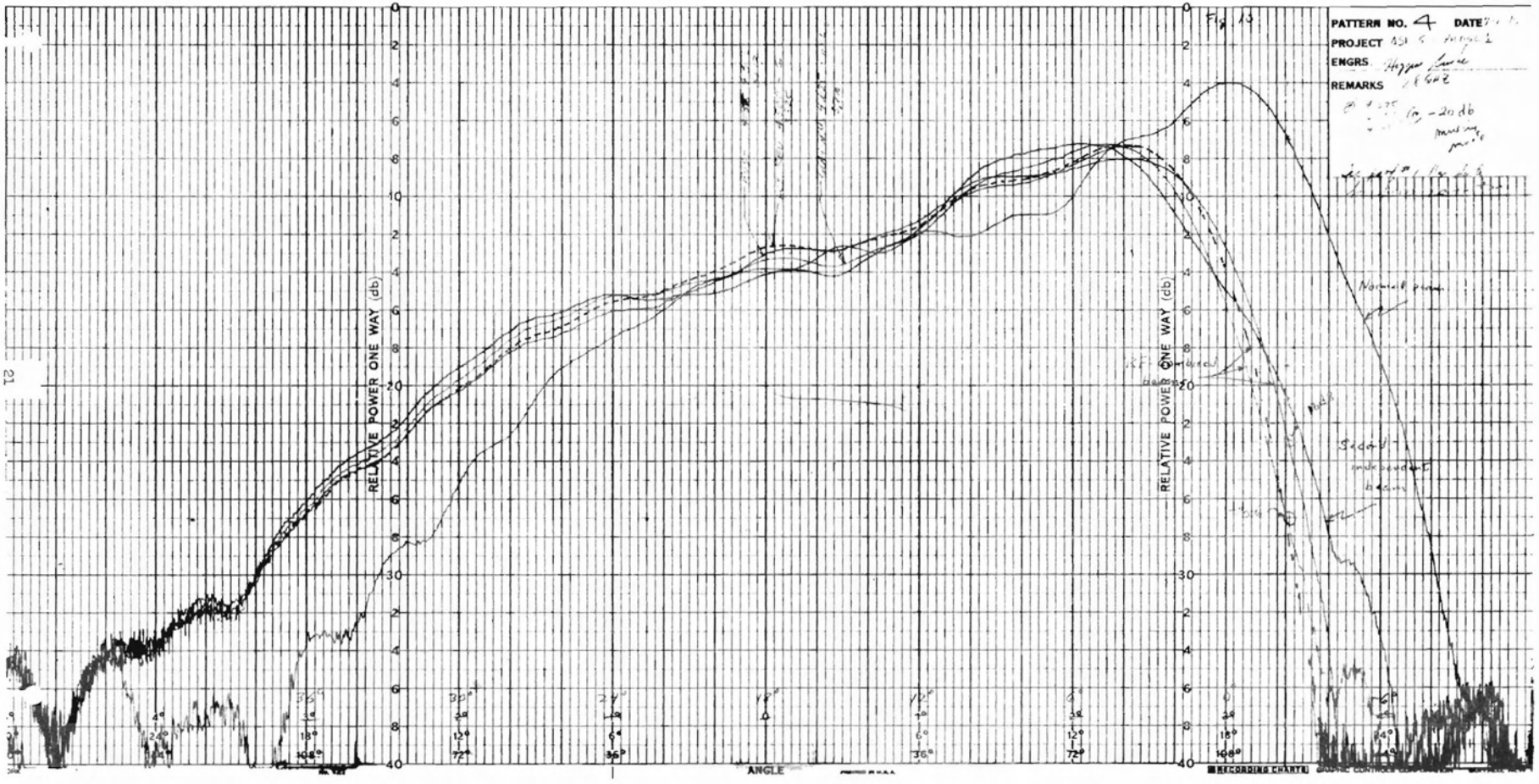

Figure 10. Measured Secondary Patterns for 3.3" x 4.7" Rectangular Aperture Second Feedhorn

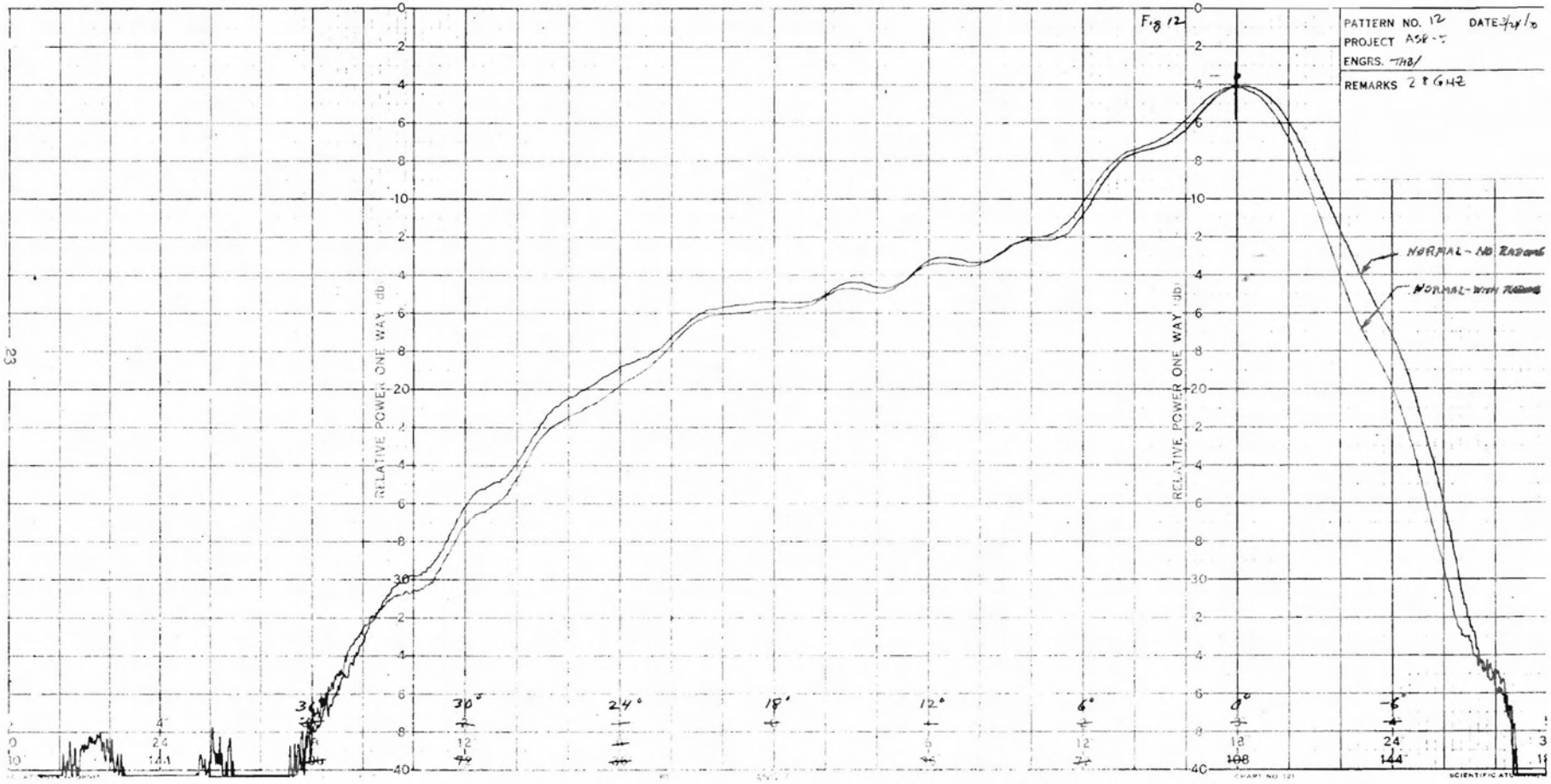

Figure 12. Measured Secondary Pattern of Normal Beam With and Without Thick (0.125") Radome.

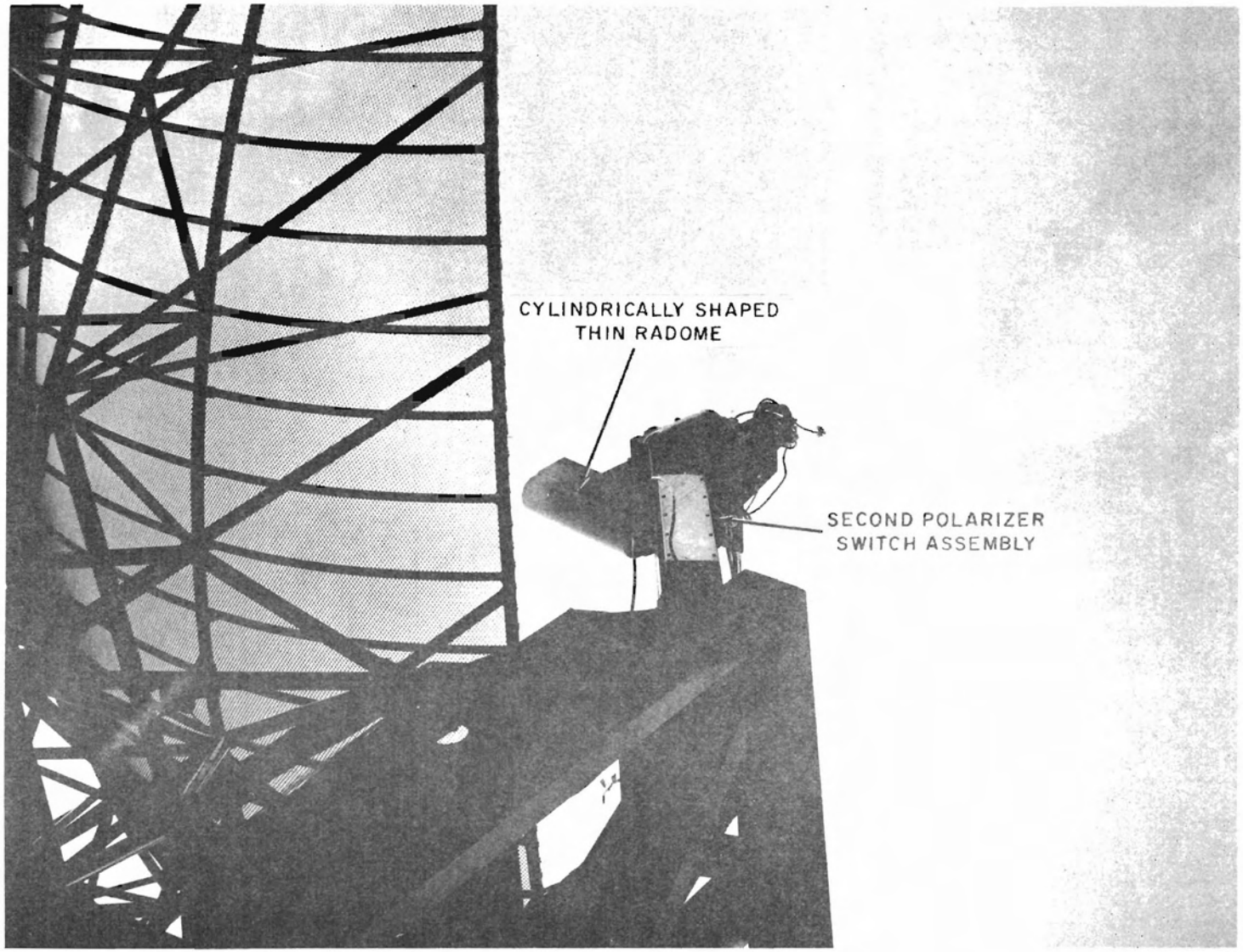

Figure 14. Oblique View of Final Feedhorn Assembly

Second Feedhorn Polarizer Switch. - Since the second feedhorn path is to be used only on reception, it is not necessary that a bulky waveguide polarizer switch (such as the normal feedhorn polarizer switch) be involved in the modified configuration. In fact, it became evident as the Phase I effort progressed that it would be extremely desirable to continue employing throughout the entire set of experimental measurements the reasonably simple and easily adjustable breadboard polarizer switch assembly that was fabricated to evaluate the primary pattern characteristics of the initial second feedhorn designs.

Figure 15 is a schematic of the polarizer switch assembly. It will be seen below in the discussion of the RF-combining network that the schematics are nearly identical. The configurations are variable power dividers.[6] For each frequency and for each beam separation condition settings of the coaxial line stretcher (phase) in the horizontal component arm and of the coaxial line stretcher (amplitude) were determined to produce the same sense circular polarization for both the second (independent) feedhorn and the normal feedhorn. Figure 16 is a photograph of the second polarizer switch assembly installed along one side of the feed support boom. Both line stretchers are driven by small motors located inside the weatherproofed package. Figure 17 is a photograph of the polarization switching circuit controls operated from the pattern recording station.

The method adopted to ensure the correct senses of circular polarization evolved as follows. Figure 18 shows a sequence of tuning adjustments for both the line stretchers (in phase and amplitude) that determine two axial ratio values of nearly unit (or an ellipticity of zero dB) when the antenna system on the pattern test pedestal is at the elevation pattern peak of the RF-combined beam. Figure 19 shows the elevation plane patterns for both these setting adjustments. One is obviously better than the other over the entire pattern shape and hence is accepted as the correct sense.

Figure 20 shows azimuth cuts at this elevation angle for the same settings and again the better pattern agrees with the sense selected as the correct sense of circular polarization.

RF-Combining Network. - The theoretical operation of the RF-combining network is depicted in Figure 21 for the receive case. Signal energy from the normal feedhorn pattern,

$$N \cdot \exp\,(j\pi/180)\,(\eta+90),$$

suitably attenuated by a factor K, and signal energy from the second feedhorn pattern,

$$S \cdot \exp\,(j\pi/180)\,(\sigma+90),$$

pass through the network components and produce at the receive output port a combined voltage signal of

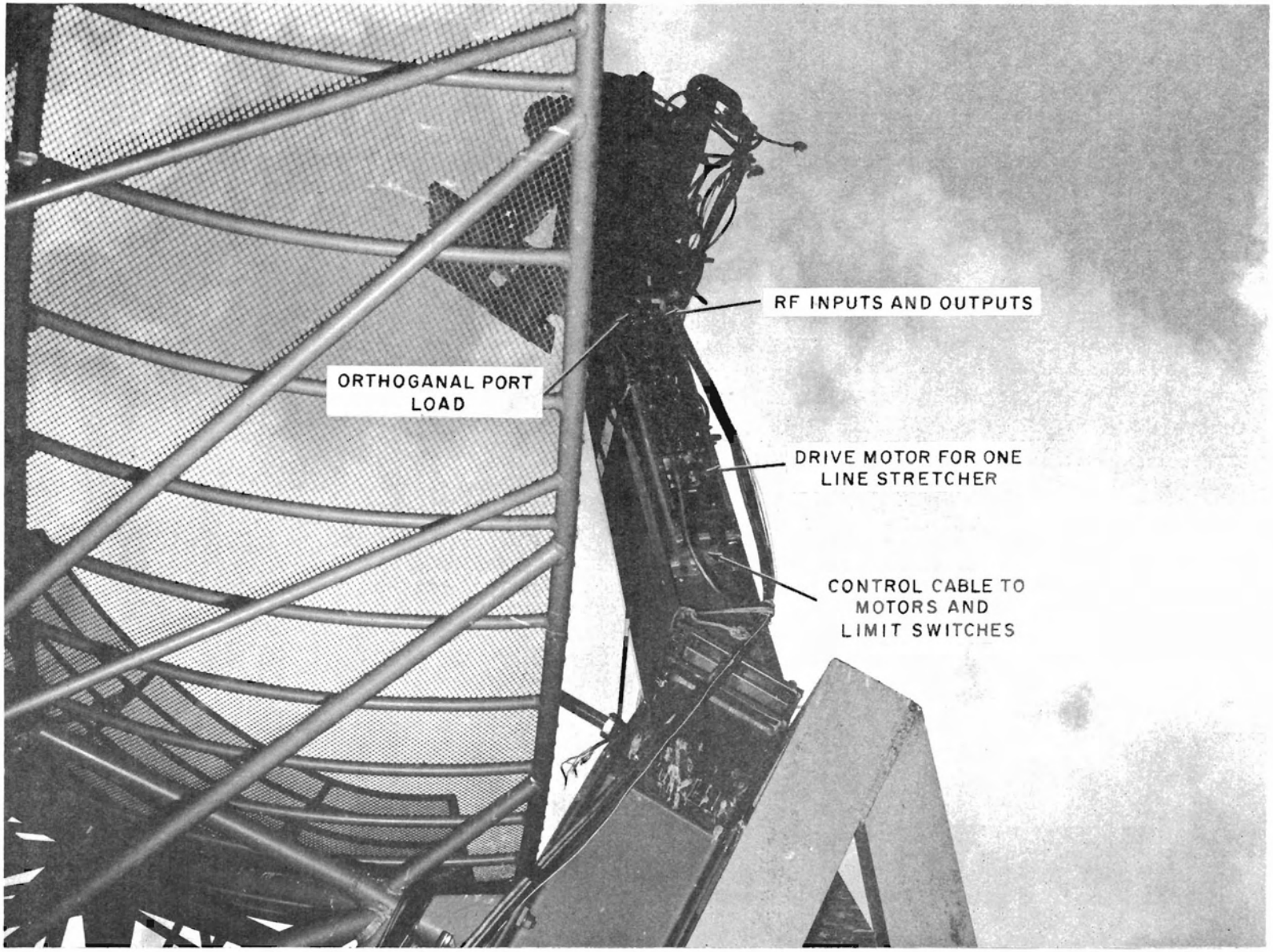

Figure 16. Photograph of Second Polarizer Switch as Installed

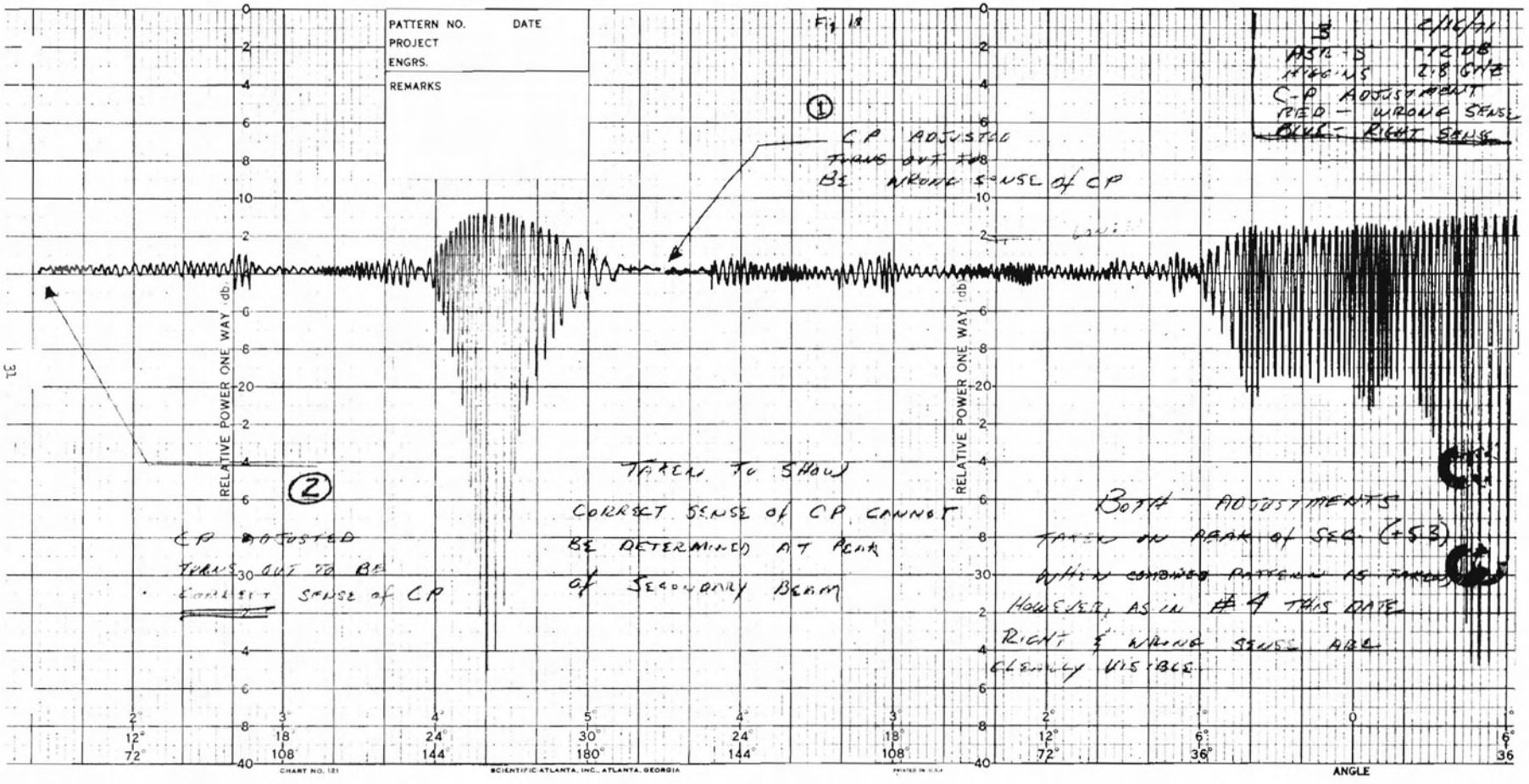

Figure 18. Adjustment Procedure for CP Settings

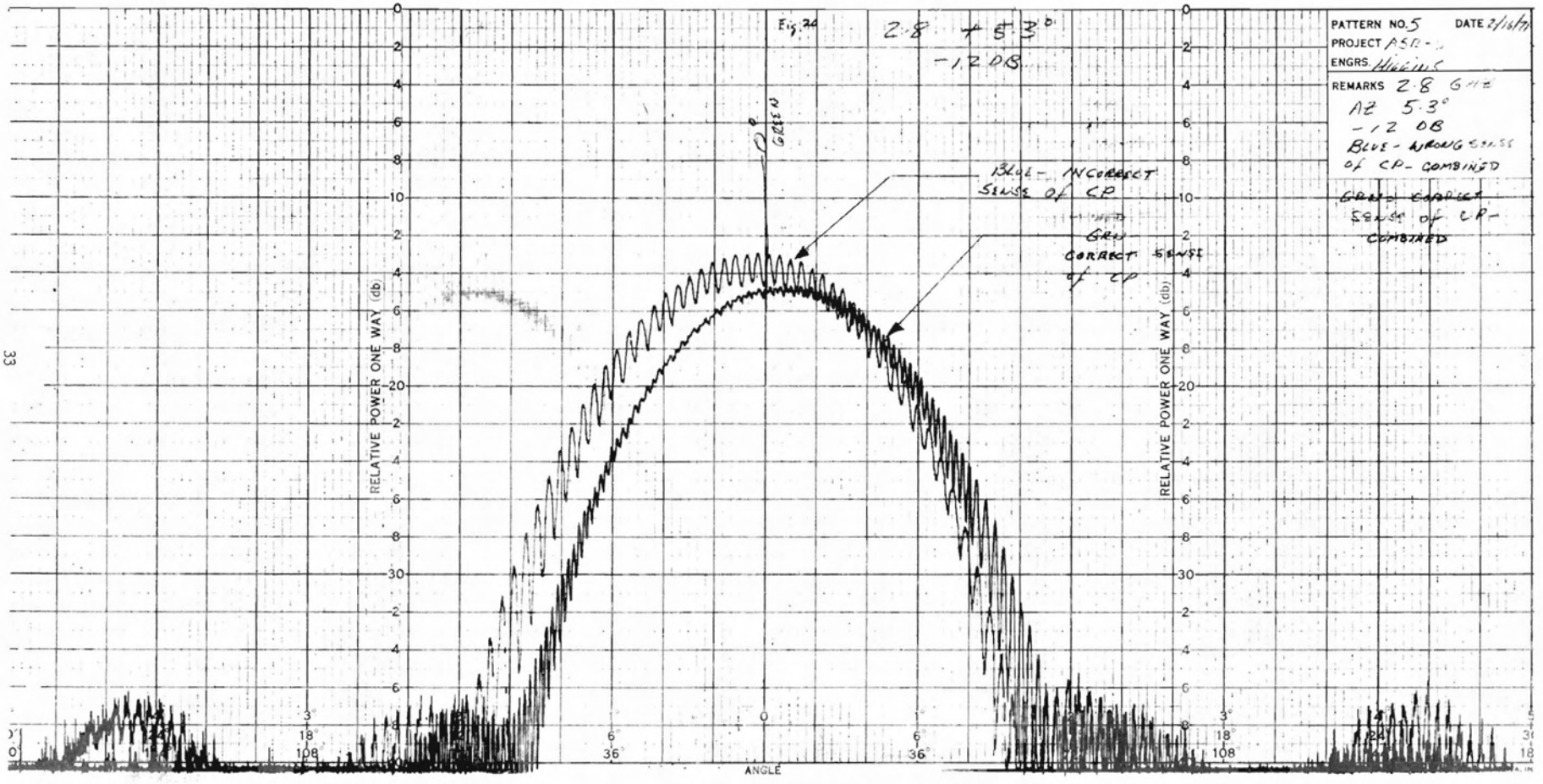

Figure 20. Measured Azimuth Cuts for CP Settings

$$R = \frac{KN}{2} \cdot \exp(j\pi\eta/180) \cdot [1 + \exp(j\pi\alpha/180)]$$

$$- \frac{jS}{2} \cdot \exp(j\pi\sigma/180) \cdot \exp(j\pi\beta/180) \cdot [1 - \exp(j\pi\alpha/180)].$$

This voltage signal can also be expressed in its real and imaginary parts as

$$R = \frac{KN}{2} [\cos(\eta) + \cos(\eta+\alpha)] + \frac{S}{2} [\sin(\sigma+\beta) - \sin(\sigma+\beta+\alpha)]$$

$$+j \frac{KN}{2} [\sin(\eta) + \sin(\eta+\alpha)] - \frac{S}{2} [\cos(\sigma+\beta) - \cos(\sigma+\beta+\alpha)]$$

Hence, the power at the receive port will be

$$P = \frac{(KN)^2}{2} (1 + \cos\alpha) - KNS \sin\alpha \cos(\sigma + \beta - \eta) + \frac{S^2}{2} (1 - \cos\alpha).$$

The existence of stationary (i. e., constant power) points in the combined secondary antenna pattern as the second feed path phase, β, is varied will occur whenever

$$\frac{dP}{d_\beta} = + KNS \sin\alpha \sin(\sigma + \beta - \eta) = 0.$$

That is, values of

$$\beta = (\eta - \sigma) \pm 180m, \quad m = 0, 1, 2, \ldots\ldots$$

produce the stationary points described in Figure 6 for

$$\alpha \neq 180m, \quad K \neq 0, \quad N \neq 0 \text{ and } S \neq 0.$$

The existence of stationary points in the combined secondary antenna pattern as the network amplitude control phaser, α, is varied will occur whenever

$$\frac{dP}{d\alpha} = \frac{(KN)^2}{2} (-\sin\alpha) - KNS (\cos\alpha) \cos(\sigma+\beta-\eta) + \frac{S^2}{2} (\sin\alpha) = 0.$$

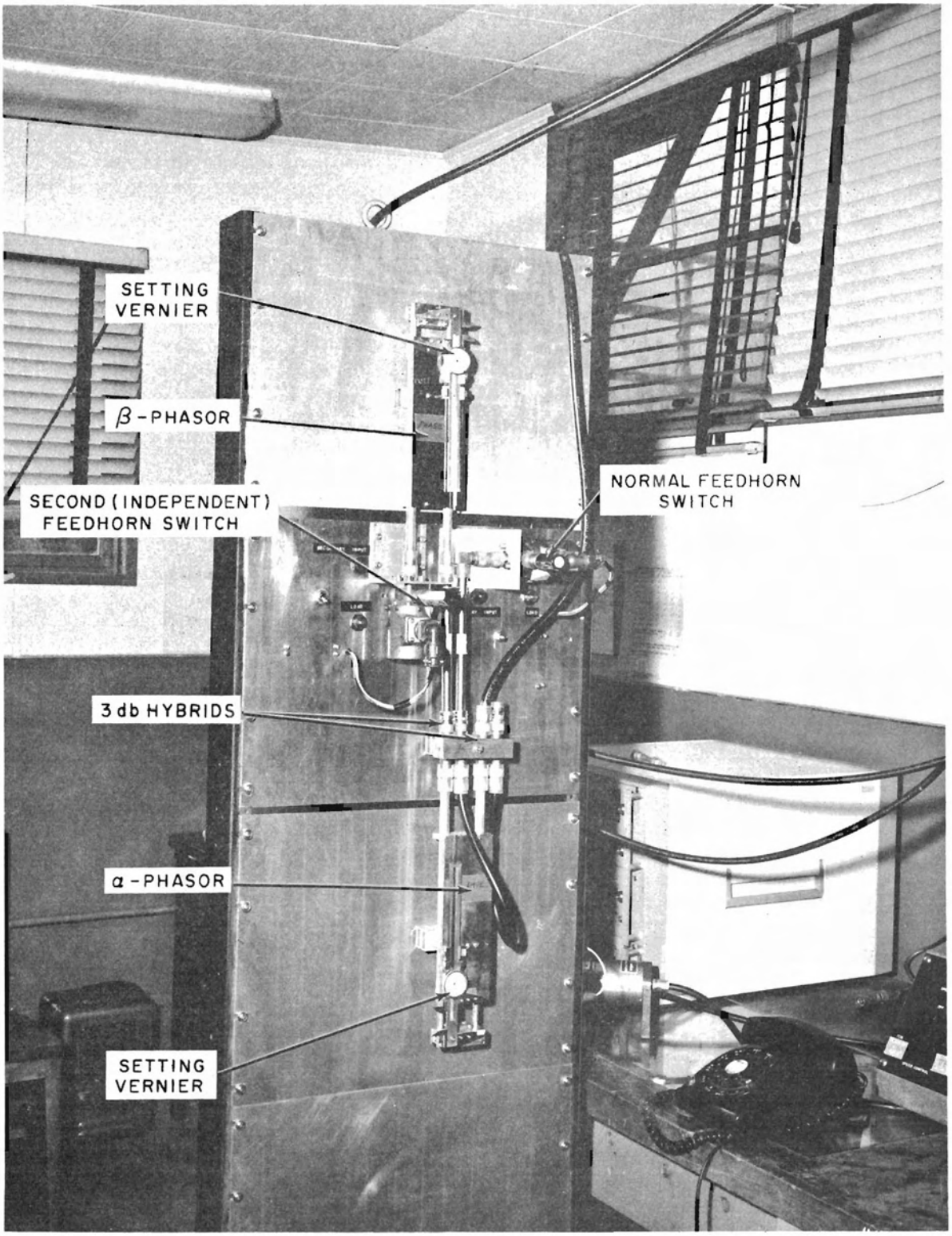

Figure 22. Photograph of RF-Combining Network Assembly

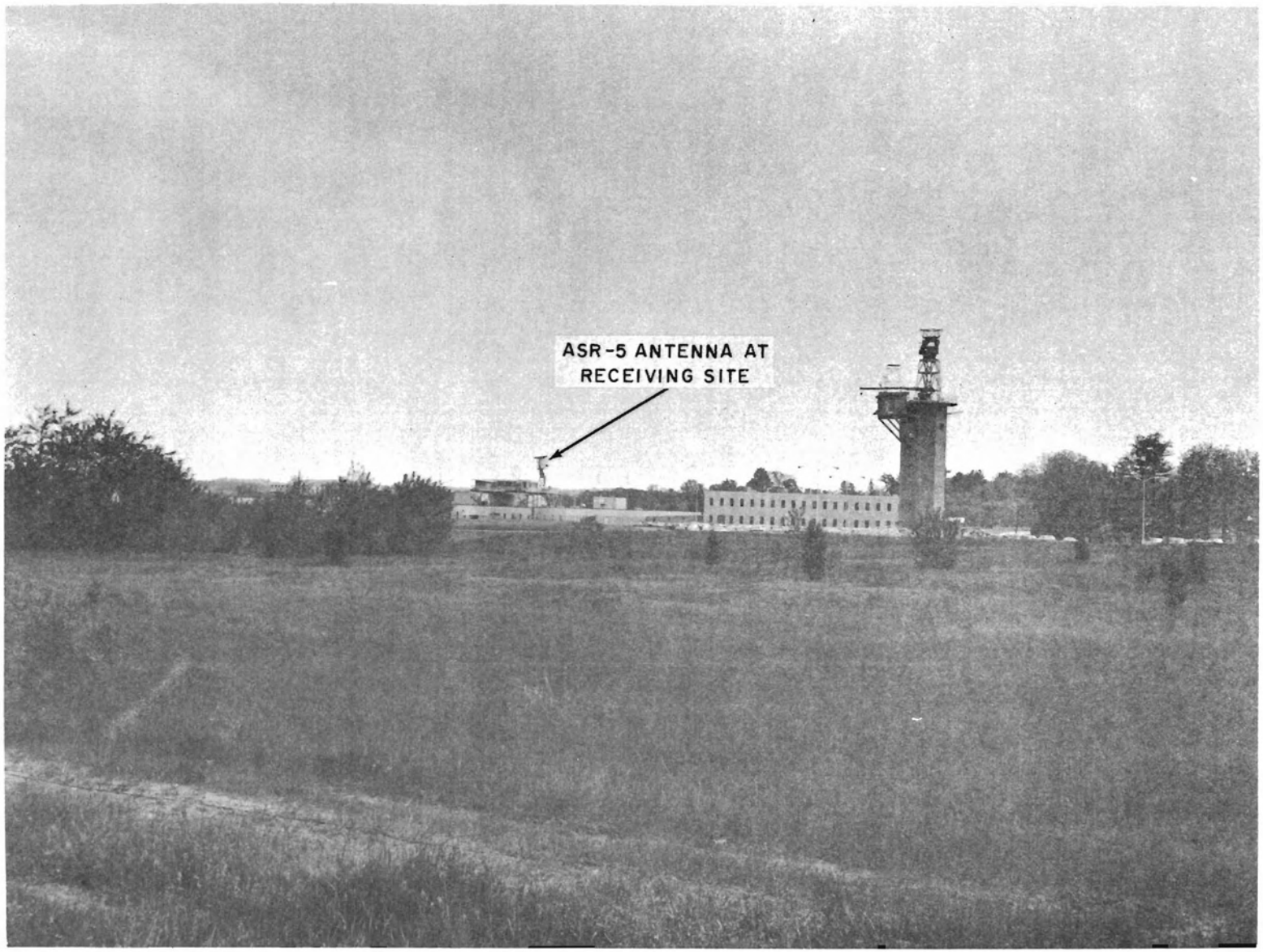

Figure 23. Sudbury Test Range (1500-foot) Looking Toward Receiving Site

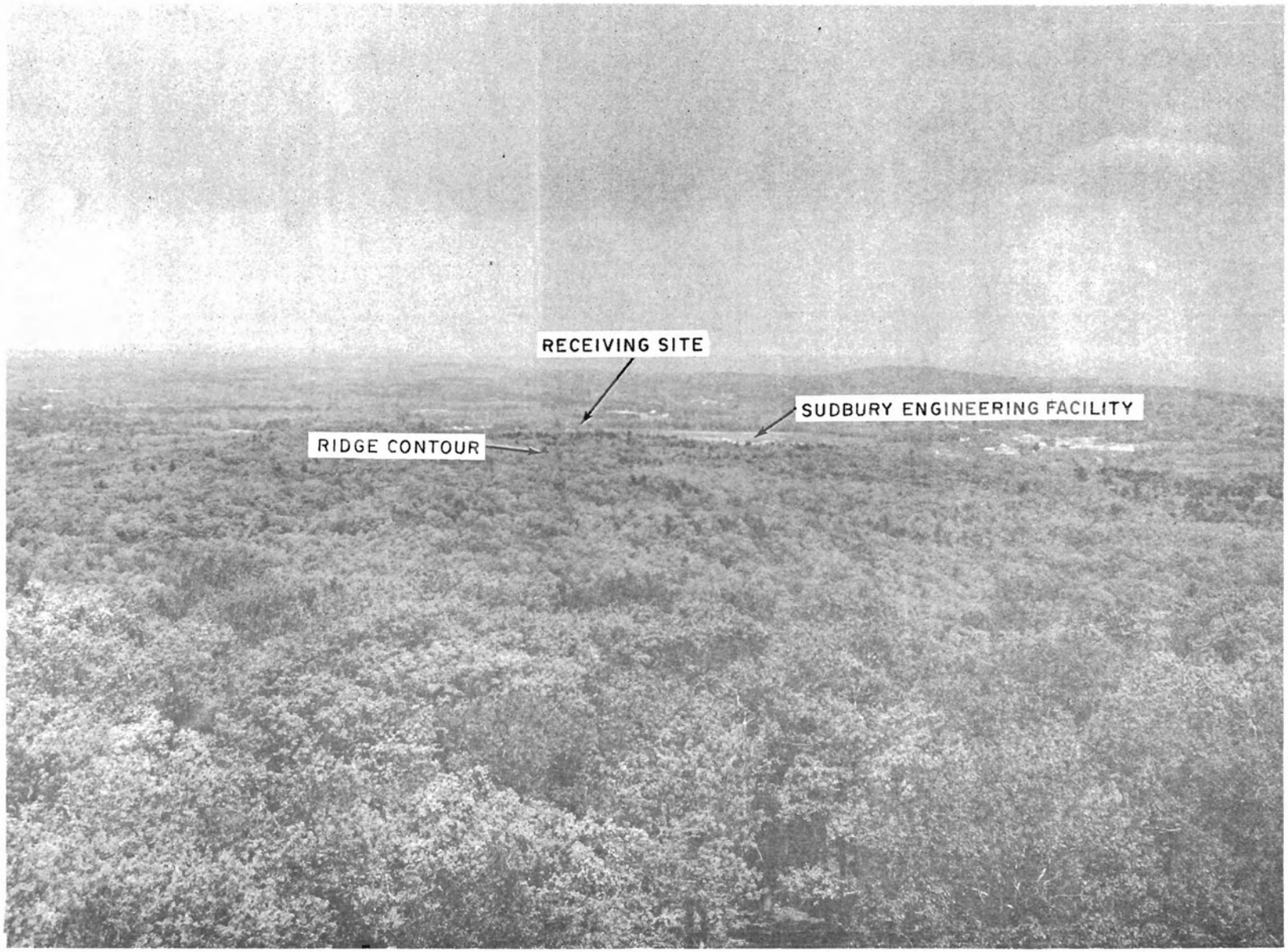

Figure 25. Nobscot-Sudbury Test Range (8000-foot) Looking Toward Receiving Site

Figure 27. Antenna Oriented in Edge-Up Position on Test Pedestal

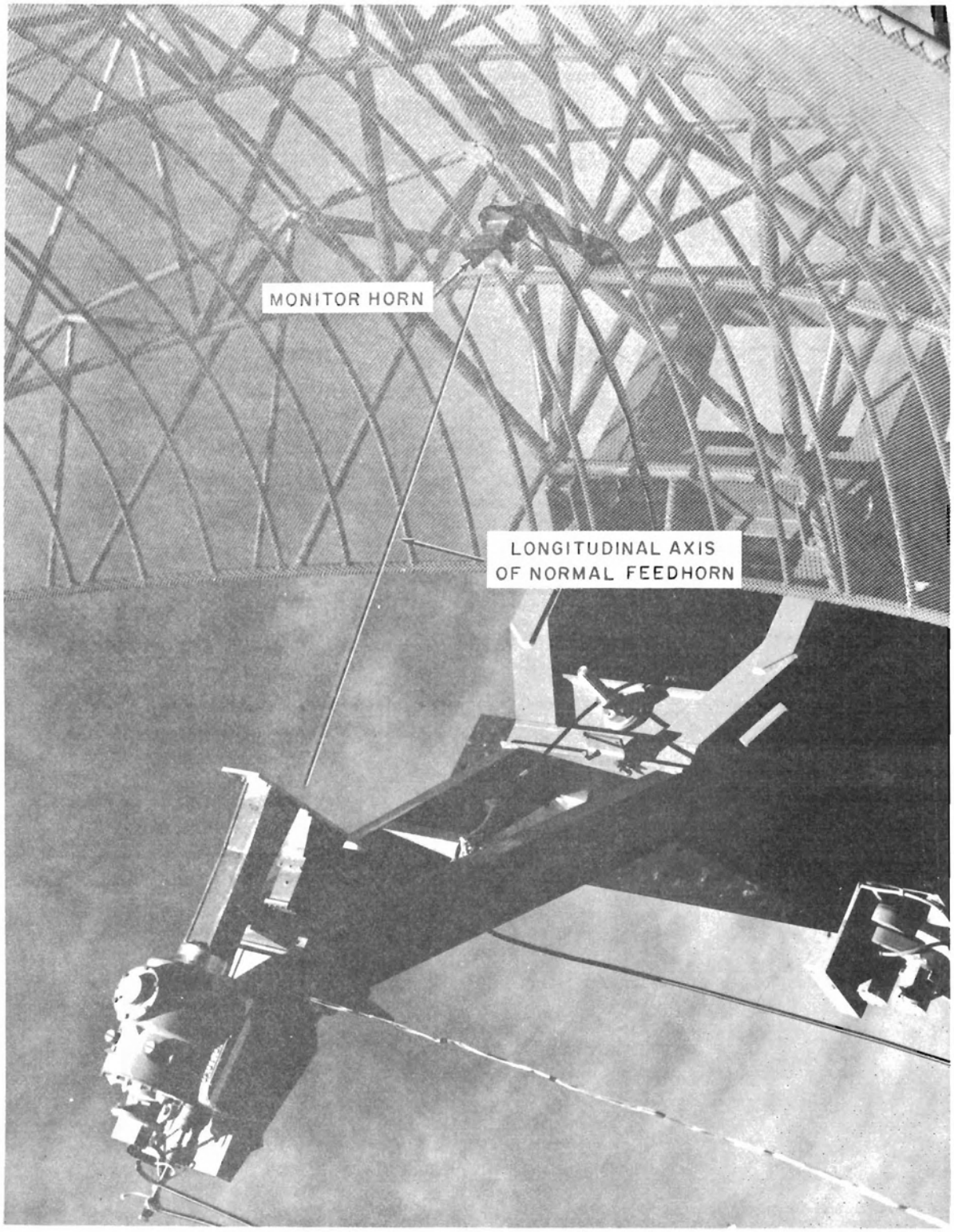

Figure 28. Monitoring Horn Mounted on Reflector

The test procedure contains two important appendices. The first describes the dual feedhorn installation and the beam separation calibration and monitoring instructions. The second appendix describes the circular polarization measurement (employing a rotating linearly polarized transmitting antenna) and data reduction instructions (including the two-way integrated cancellation ratio expressions).

Pattern Data. - When good circular polarization had been obtained with the 3.3" x 4.7" internal-finned aperture second feedhorn independently, the preliminary secondary patterns shown in Figure 30 through 38 were recorded for the three frequencies and the three beam separation conditions. The vernier readings for the α- and β- phasors associated with each of these linearly polarized patterns can be seen on each chart. A similar set of patterns were measured to obtain the α- and β- phasor vernier readings for circular polarization. It happens that the amplitude control α- phasor settings were identical for linear and circular polarization. These settings were unchanged throughout the pattern measurement procedure. The β- phasor readings were, of course different by an amount determined to be primarily due to the electrical path lengths in the two polarizer switches being different by nature of their designs. During the pattern measurement procedure constant differences between the β- phasor settings and the corresponding vernier readings obtained by nulling out a test signal from the monitor horn through the RF-combiner were maintained.

Test Data Evaluation. - As mentioned above, a very large amount of test data has been recorded on the 586-plus pattern charts. Many of the measurements were obviously intended only as a check (1) that no unexpected phenomena occurred in implementing the RF-combining technique of varying the second beam pattern and (2) that only minimum degradation shall have occurred for the normal feed pattern characteristics.

A small selection of the measured pattern charts is included in this section to show typical final results for the modified antenna system. The selection has arbitrarily been restricted to the 12 dB separation condition at 2.8 GHz on the assumption that this is the worst combining situation. Discussion of these charts herein follows the listed order of antenna parameters and/or characteristics given above.

(1) Figure 39 verifies that the normal feed elevation plane pattern peak (by a -1 dB definition) shifts less than 0.04° across the frequency band.

(2) Figure 40 verifies that backlobe radiation levels for both the normal and second feed elevation plane patterns are at least 28 dB down.

(3) Figure 41 shows the elevation plane pattern beamshapes for both the normal feed and the second feed (12 dB condition). Also shown on the chart are key points from the elevation plane radiation pattern specification for the unmodified antenna (FAA-R-864c, February 9, 1968, Airport Surveillance Radar). Note the normal feed pattern continues to meet this shape.

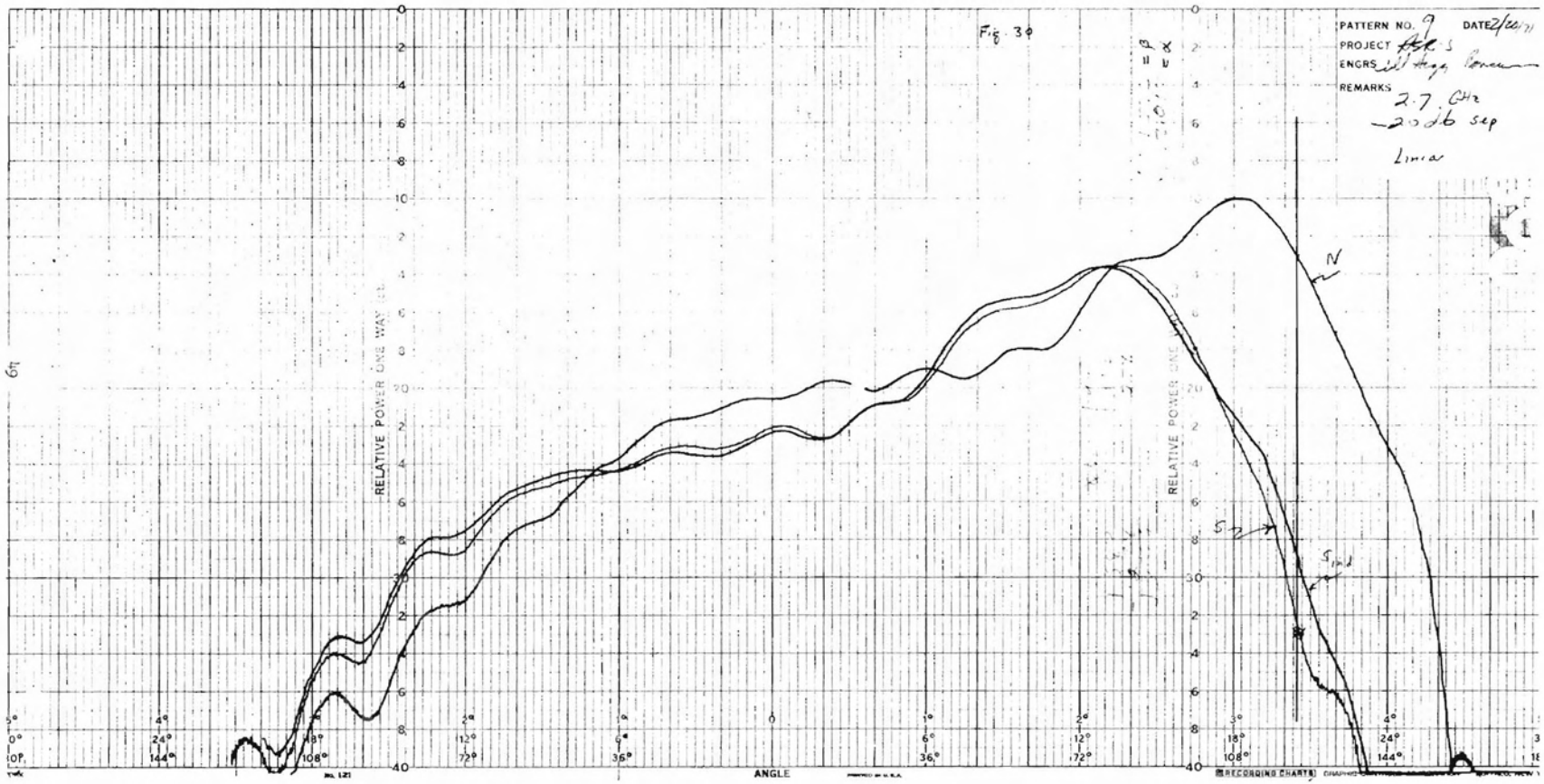

Figure 31. Calibration Pattern for -20 dB Separation at 2.7 GHz

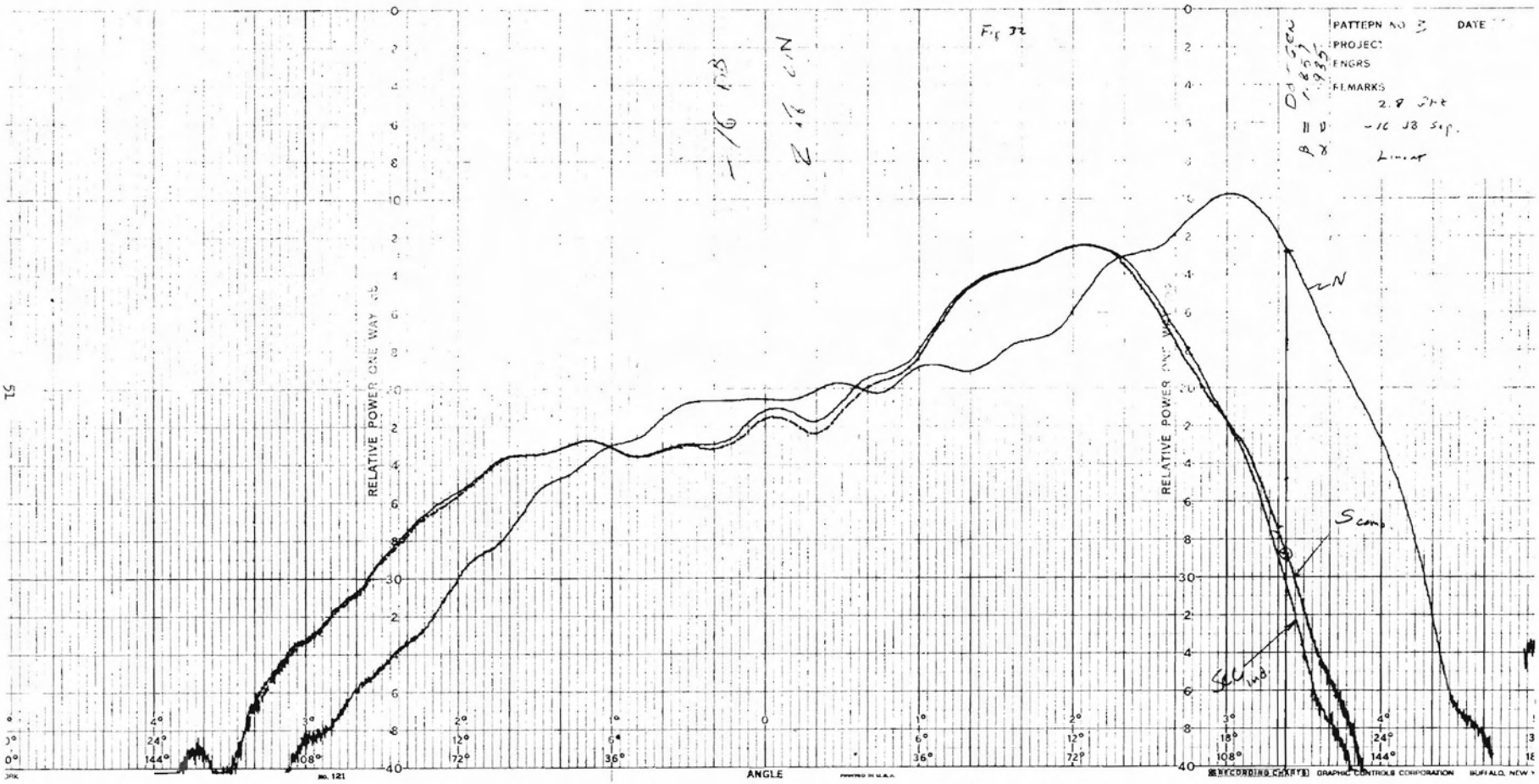

Figure 33. Calibration Pattern for -16 dB Separation at 2.8 GHz

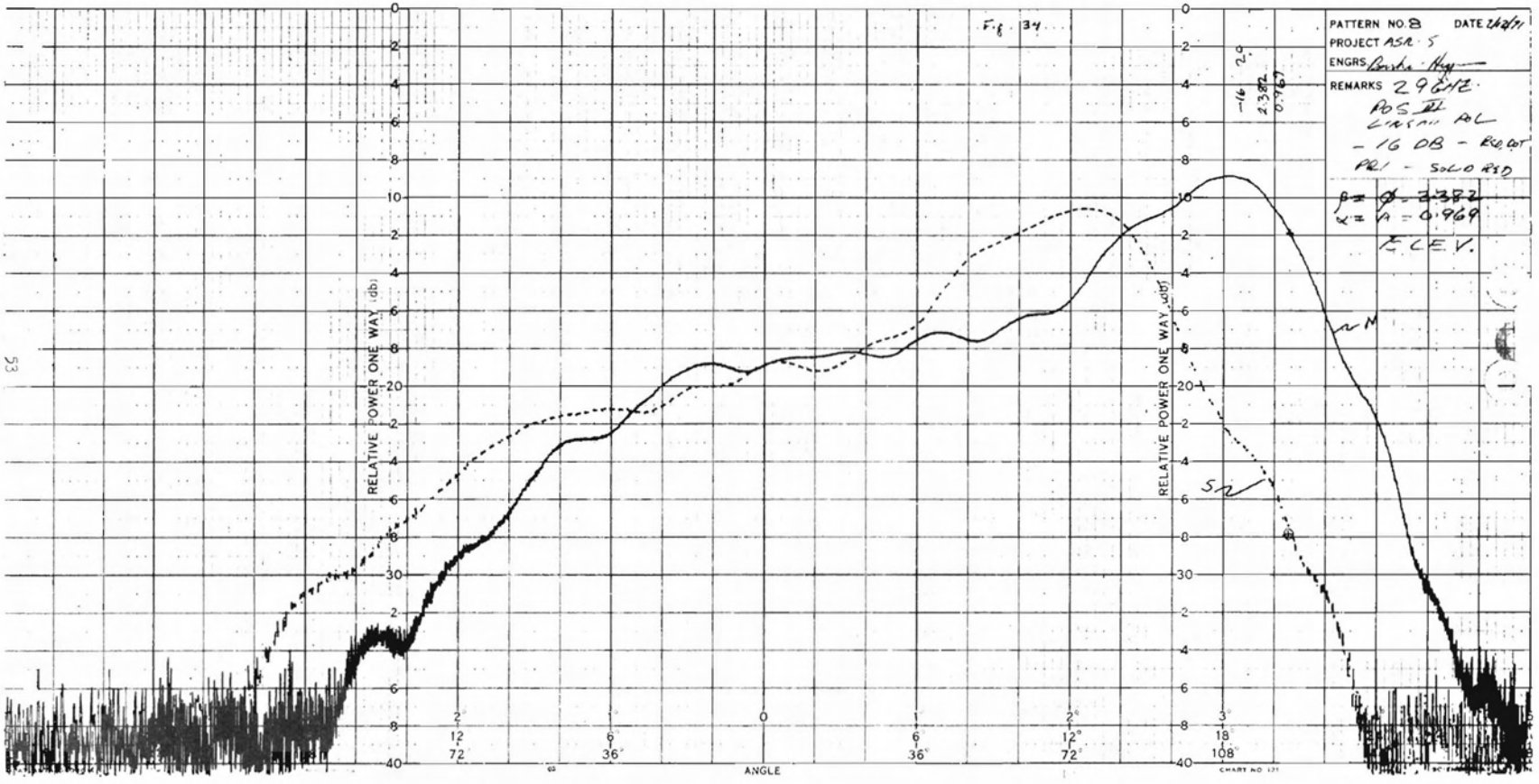

Figure 35. Calibration Pattern for -16 dB Separation at 2.9 GHz

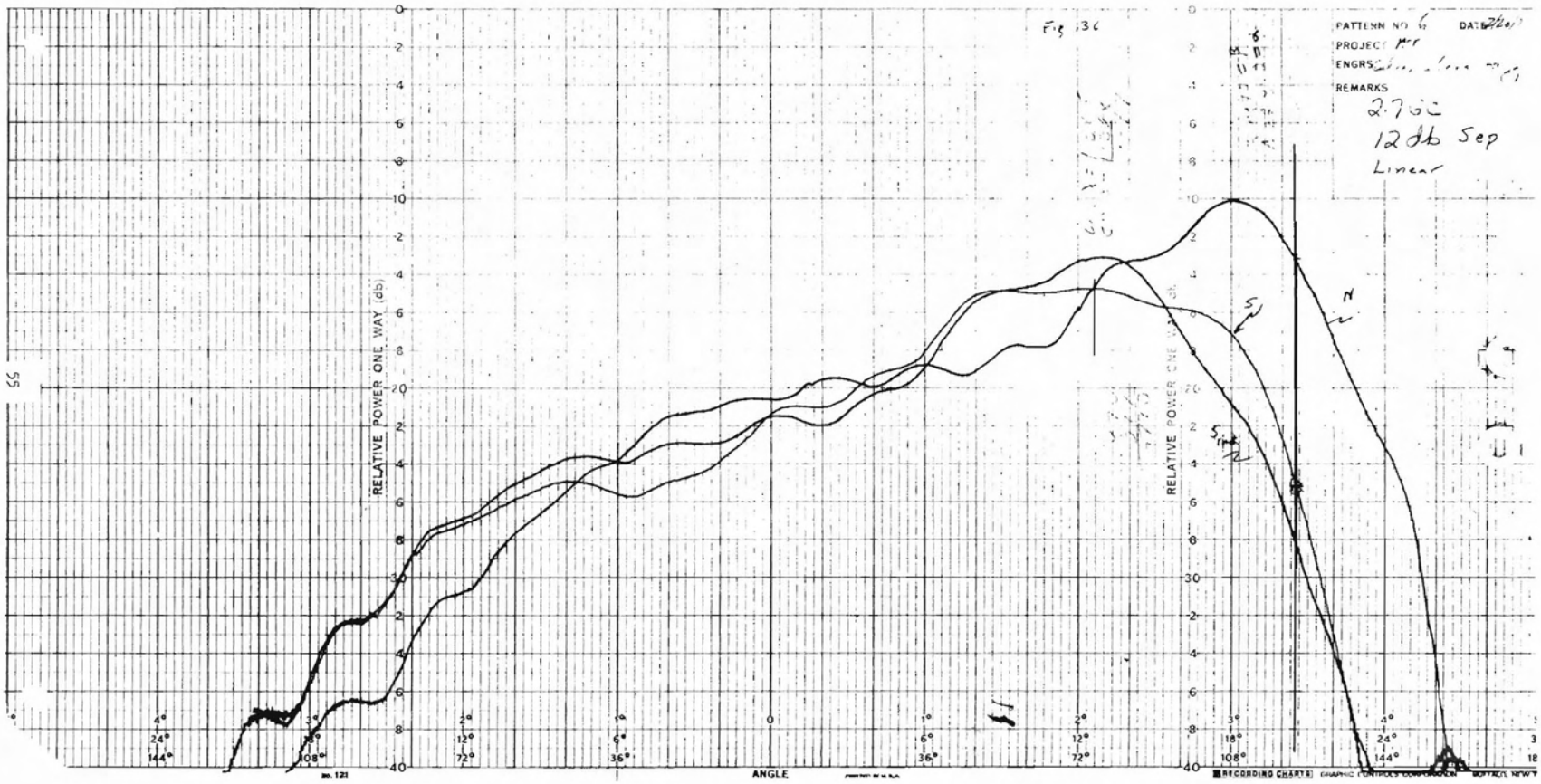

Figure 37. Calibration Pattern for -12 dB Separation at 2.7 GHz

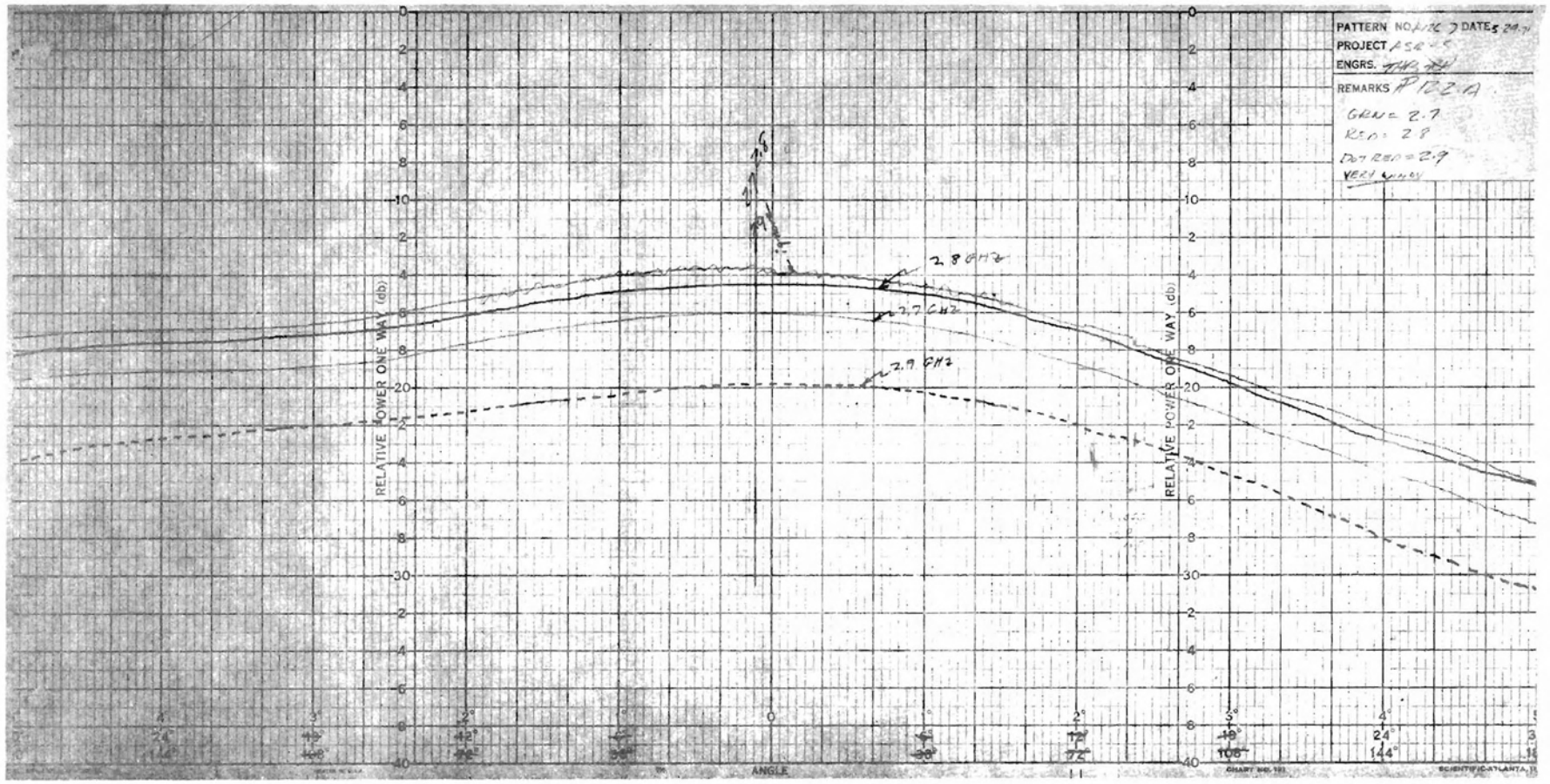

Figure 39. Normal Feed Elevation Plane
Pattern Peak versus Frequency

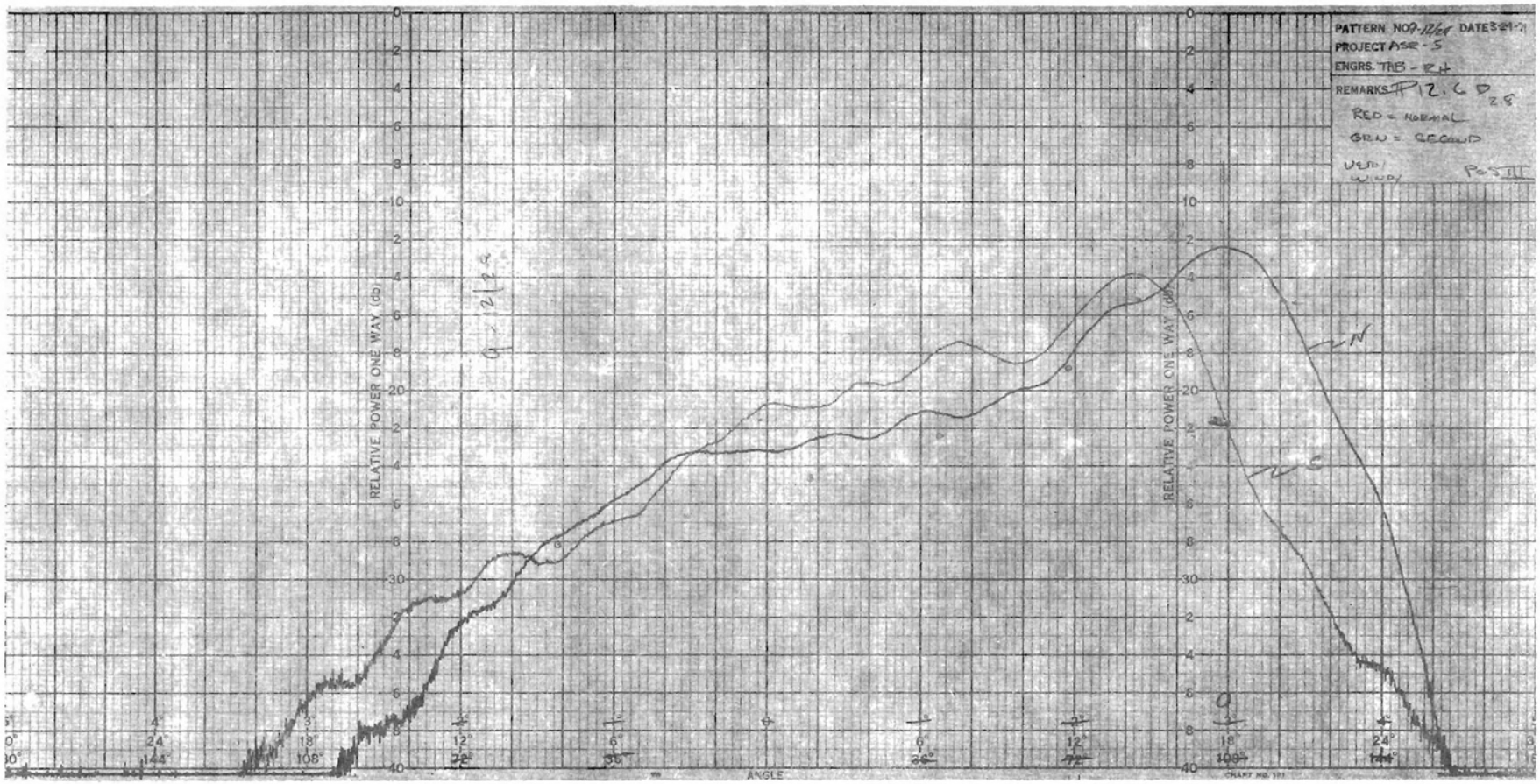

Figure 41. Elevation Plane Patterns for Beamshape Evaluation

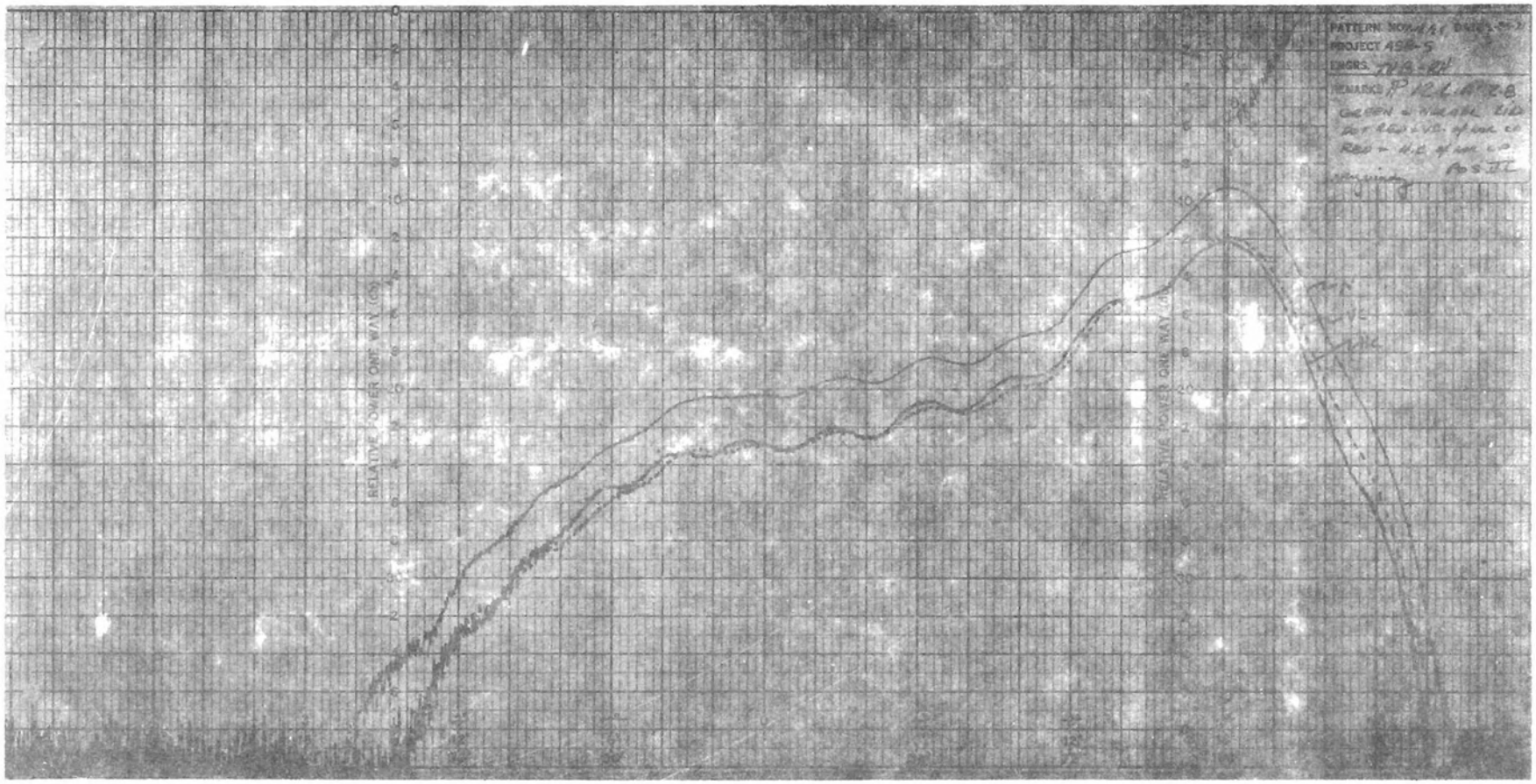

Figure 42. Normal Feed Elevation Plane Polarization Components

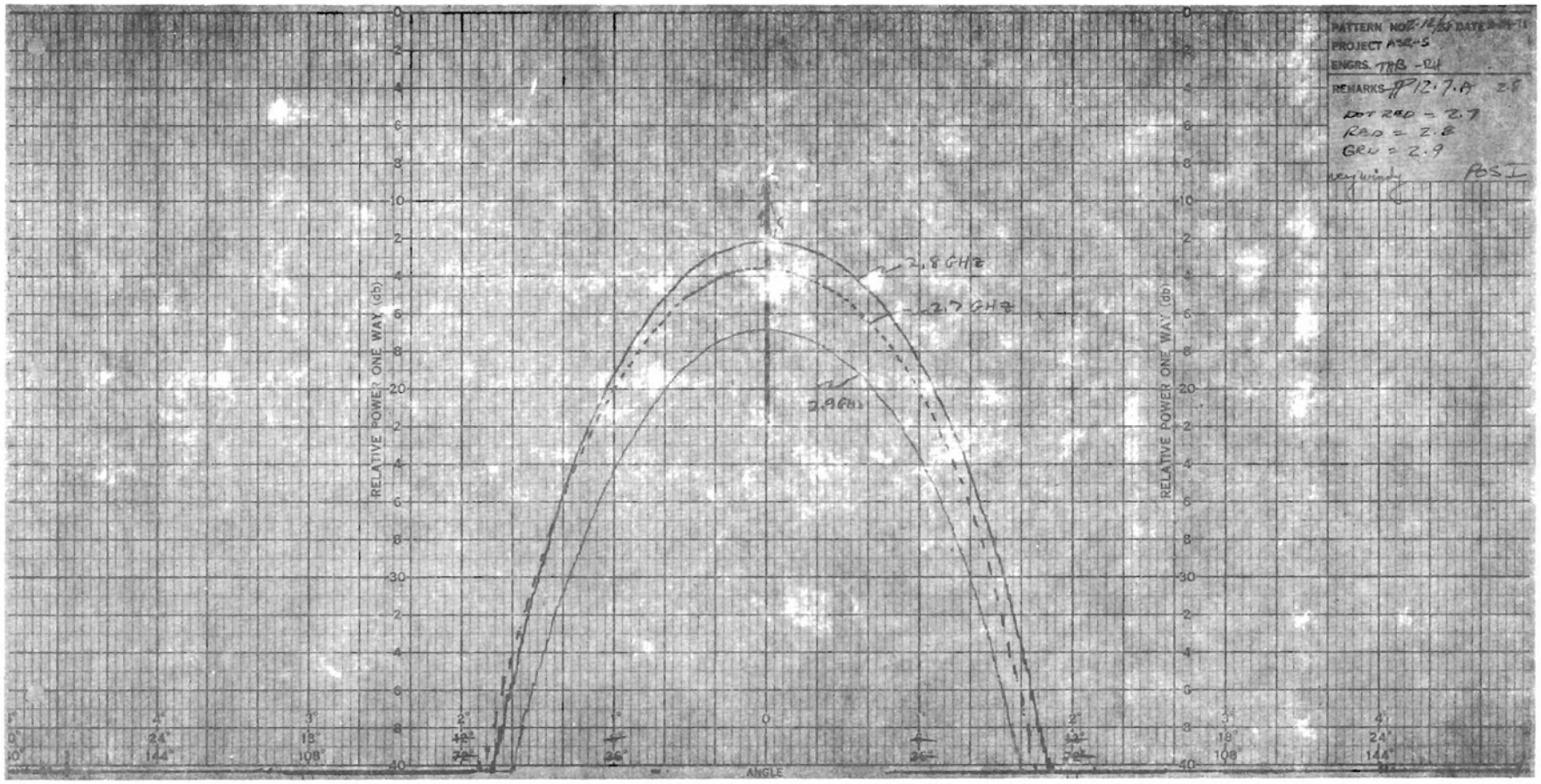

Figure 44. Normal Feed Azimuth Plane Pattern Peak versus Frequency

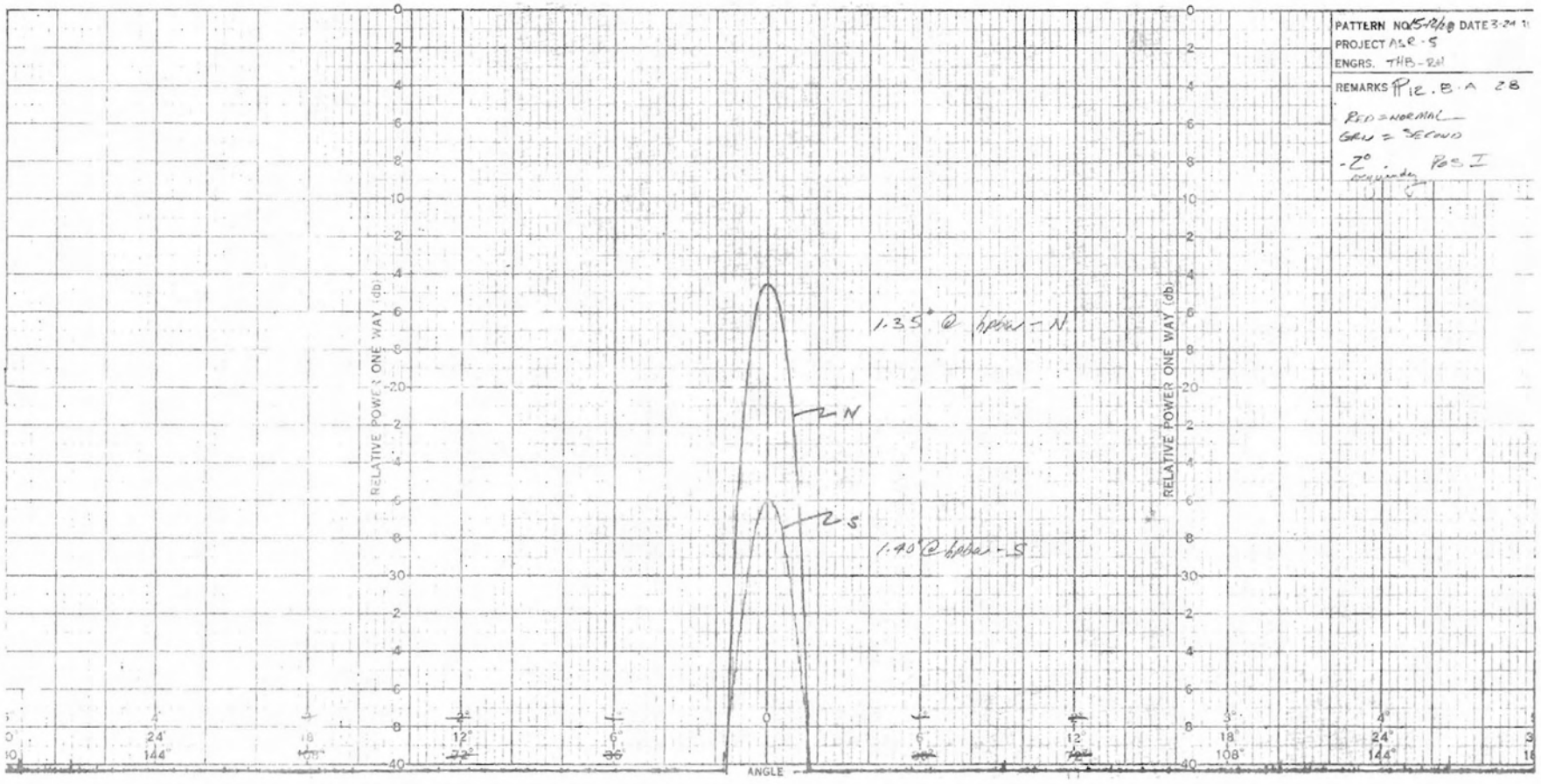

Figure 46. Azimuth Plane Cuts at -2° in Elevation

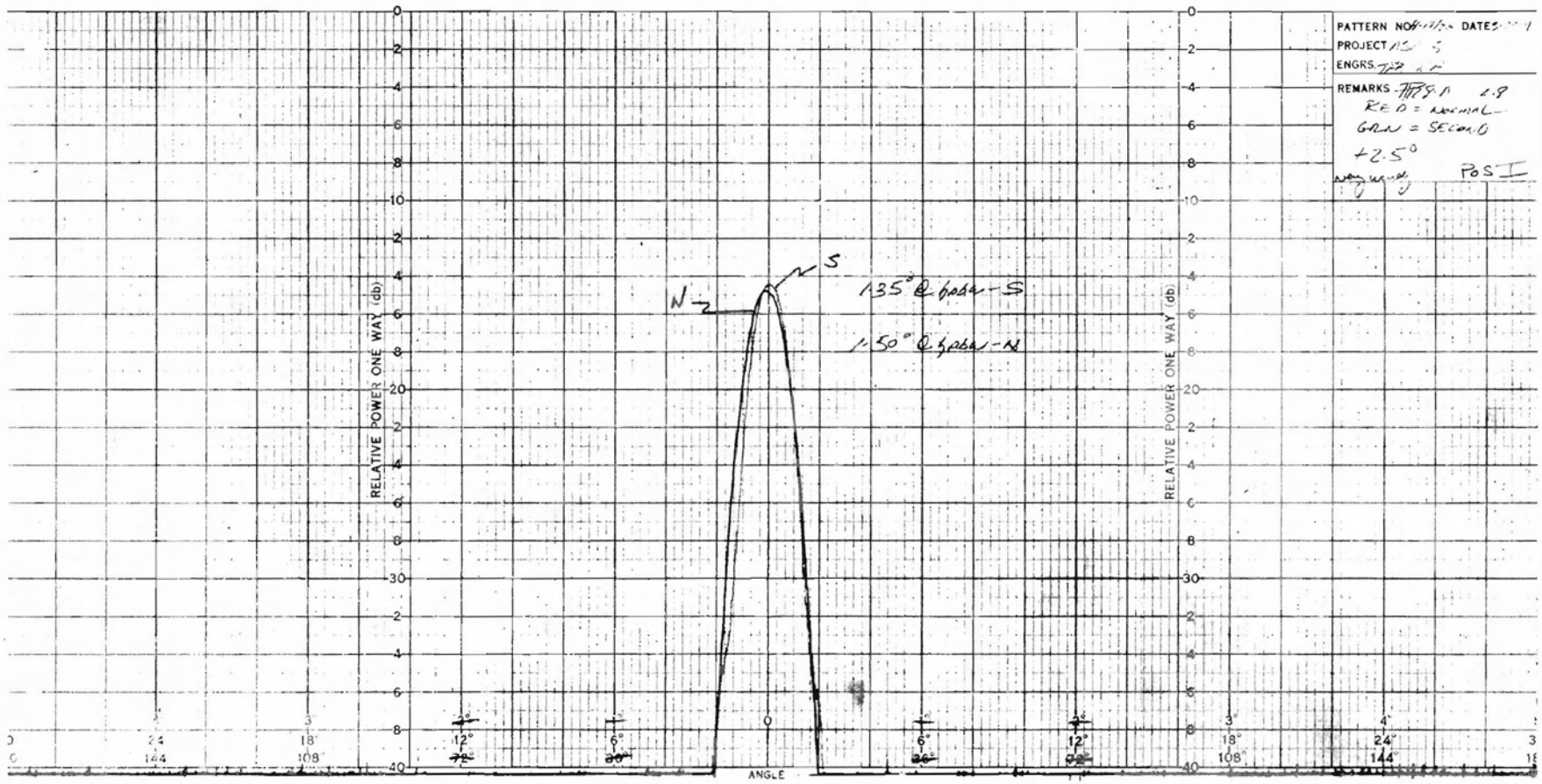

Figure 48. Azimuth Plane Cuts at 2.5° in Elevation

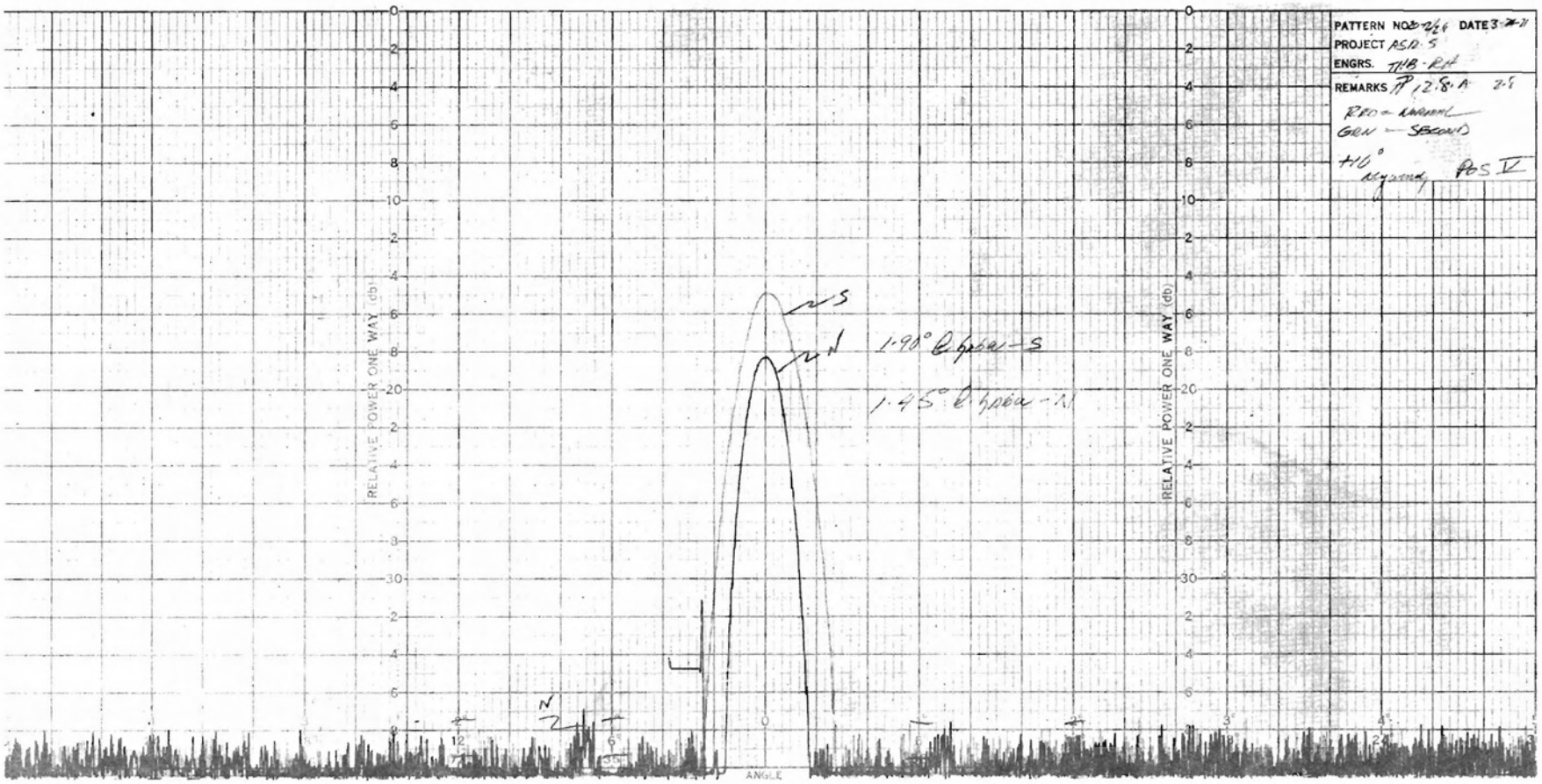

Figure 50. Azimuth Plane Cuts at 10° in Elevation

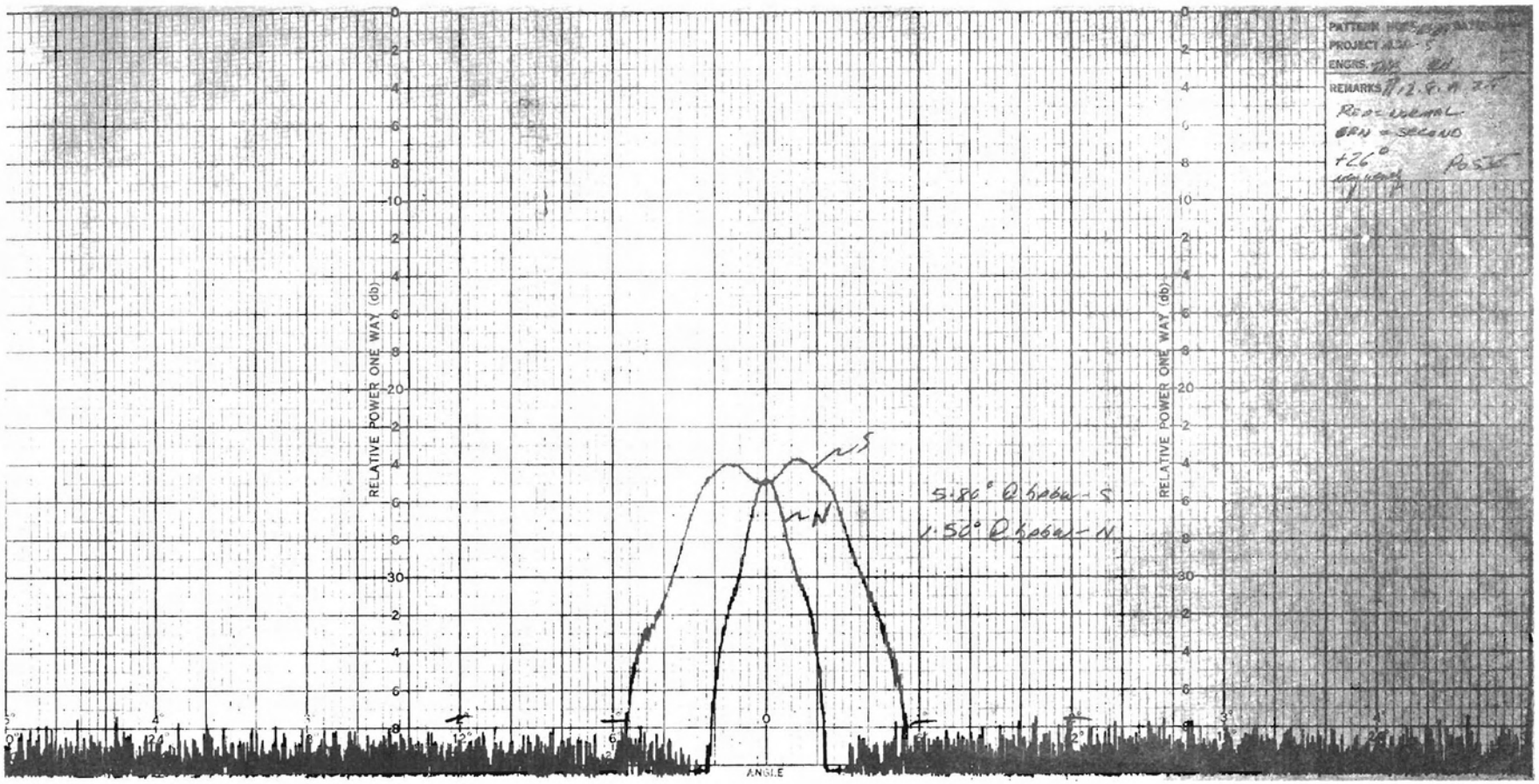

Figure 52. Azimuth Plane Cuts at 26° in Elevation

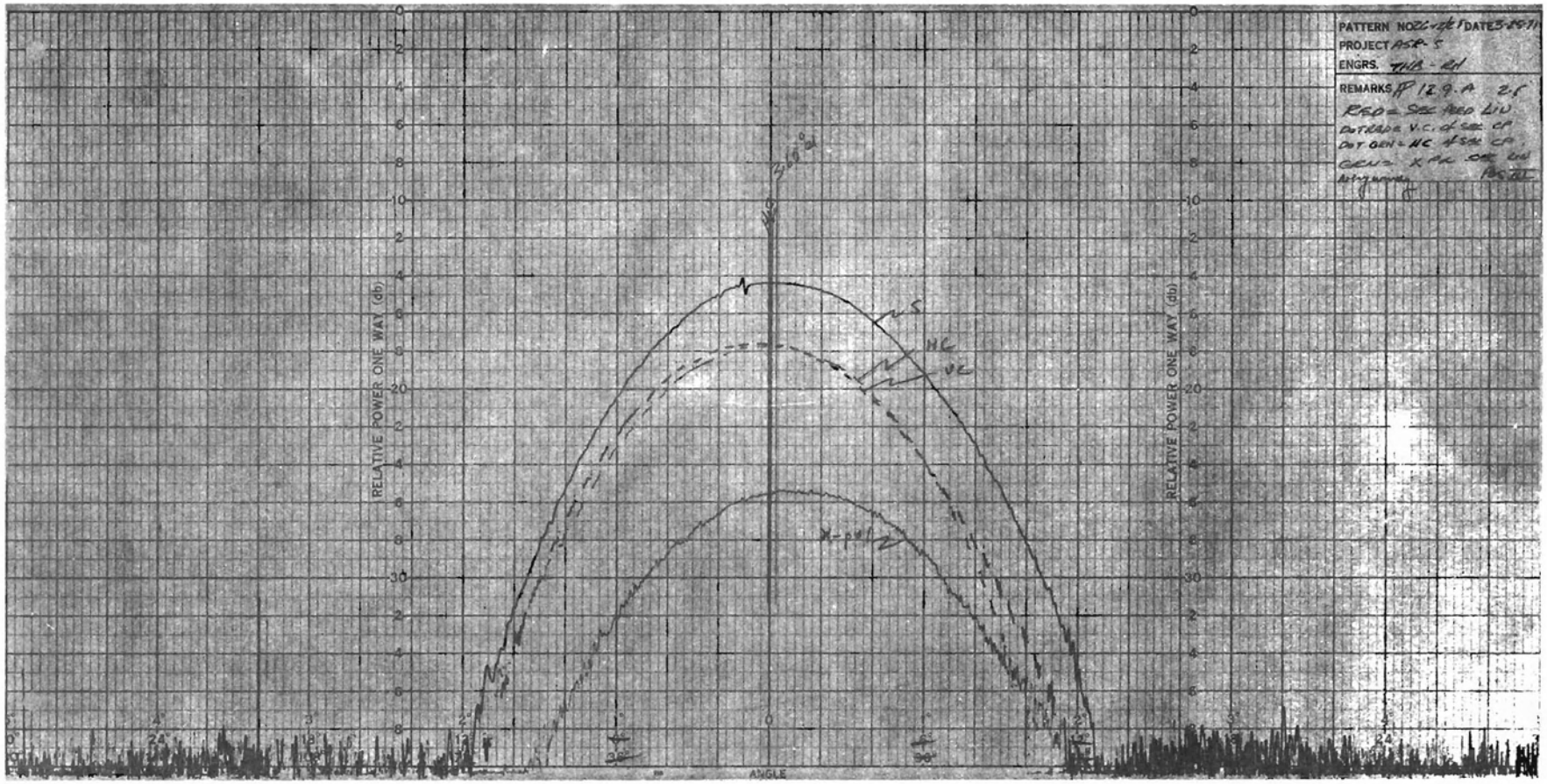

Figure 54. Second Feed Azimuth Plane Polarization Components

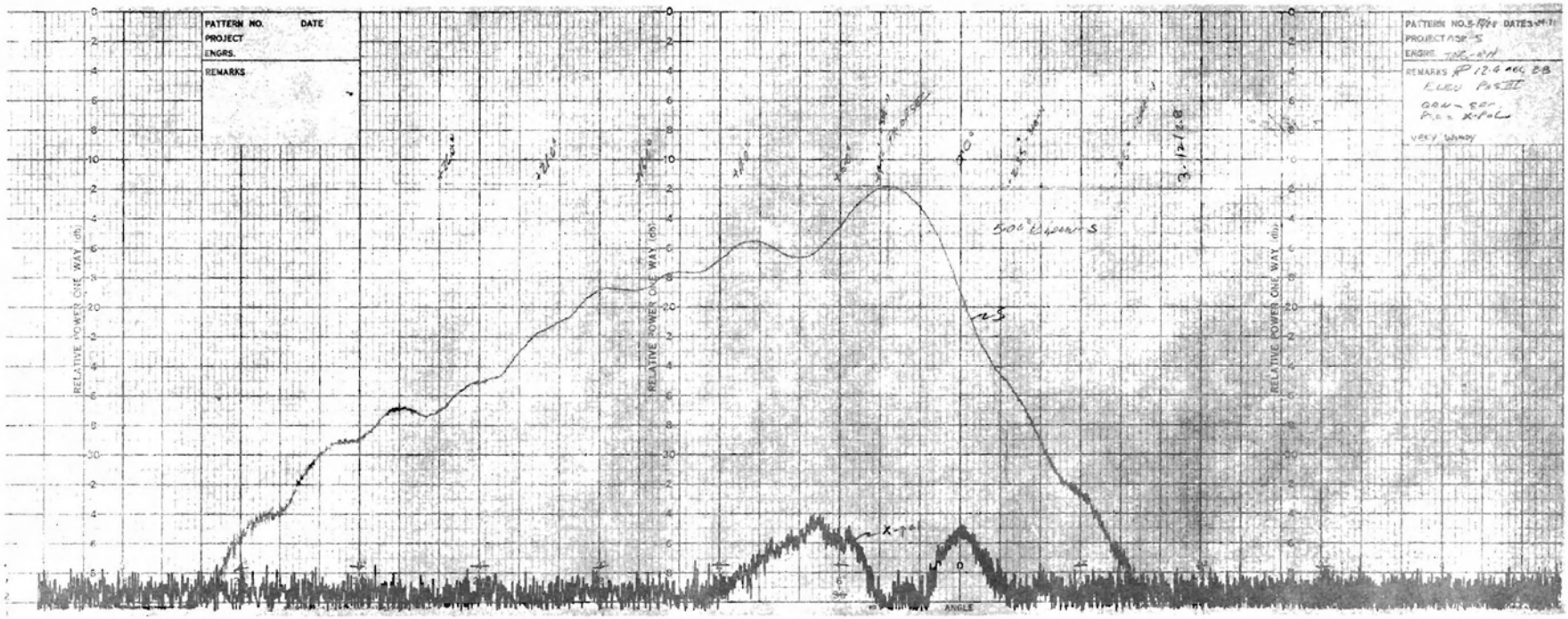

Figure 56. Second Feed Elevation Plane Cross-Polarization Level

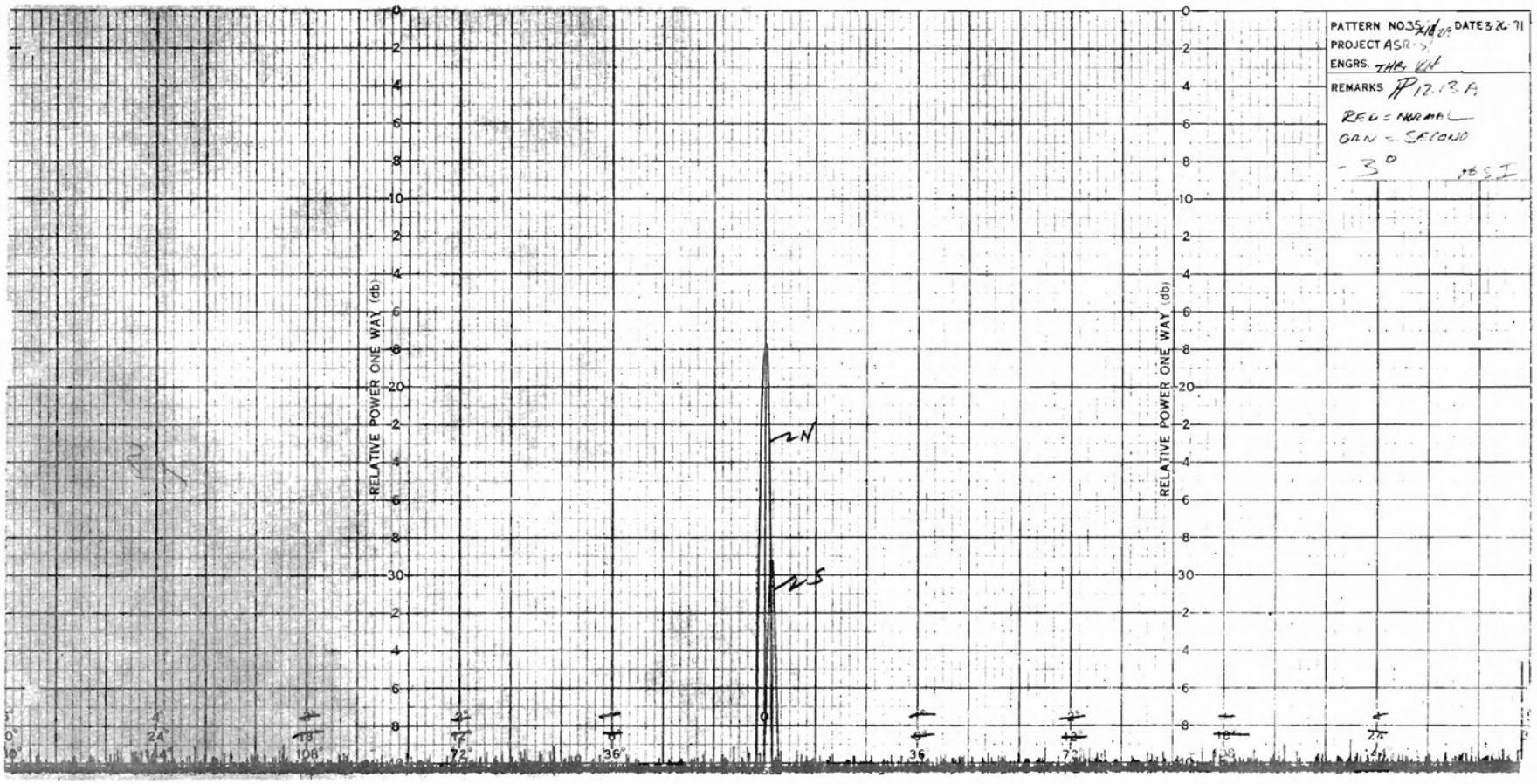

Figure 58. Azimuth Plane Pattern for Backlobe Evaluation (at -3°)

The added pattern charts which show the consistency of the second feed elevation plane pattern across the frequency band at 25 MHz intervals are included herein as Figures 59 and 60. The α - and β - phasor vernier settings for the RF-combiner were linearly interpolated for the 25 MHz frequency steps between 2.7 GHz and 2.8 GHz and between 2.8 GHz and 2.9 GHz. It was noted during this process that it was vital that the electrical path lengths from each feedhorn to its respective RF-combiner input port be an equal number of integral wavelengths. Bearing in mind that the normal feed pattern at frequencies other than 2.8 GHz will fluctuate by possibly several tenths of a dB about the 2.8 GHz pattern shown in both figures, it is observed that the second feed patterns for a 12 dB separation condition undoubtedly remain within ± 1 dB of the 12 dB condition over the frequency band.

Circular polarization performance for this type of system is of such importance that graphs are presented herein of the calculated data showing elevation and azimuth plane ICR values for the composite two-way beam (i.e., transmission on the normal beam and reception on the second beam) for the nine sets of measured patterns. Figure 61 is a plot of the elevation plane ICR values showing the composite beam ICR value in relation to the best and worst cases of orientation for the polarization ellipses of the normal beam and of the second beam. Figures 62 through 70 are similar plots for the azimuth plane pattern cuts throughout the region of interest in elevation.

A small selection of the measured patterns providing the input data for the ICR value computations is included herein. Again the selection is limited to the 12 dB condition at 2.8 GHz. Figures 71 and 72 are the elevation plane patterns for the normal feed and the second feed (12 dB condition), respectively, when the polarizer switches are set for circular polarization and the transmitting antenna is operating with a linearly polarized rotating signal.

Close examination of the recorded patterns reveals points where the recording pen was momentarily lifted from the chart paper when one of the transmitter antenna vertical polarization positions of the rotating cycle occurred. Four calibration points are also seen on the charts. These points were employed to properly orient each chart for digitizing (onto punched data cards for computer input with an Auto-trol Model 5800 digitizer) the maximum power envelope, the minimum power envelope, and the angular location of each vertical polarization position. The polarization tilt angle, τ , required in the composite beam ICR value calculations was interpolated within the computer program from the vertical polarization position input data.

Figures 73 through 86 are azimuth pattern cuts at various elevation angles between -4° and $\pm 26^{\circ}$ for both the normal feed and the second feed (12 dB condition) under the rotating linear transmitting antenna setup.

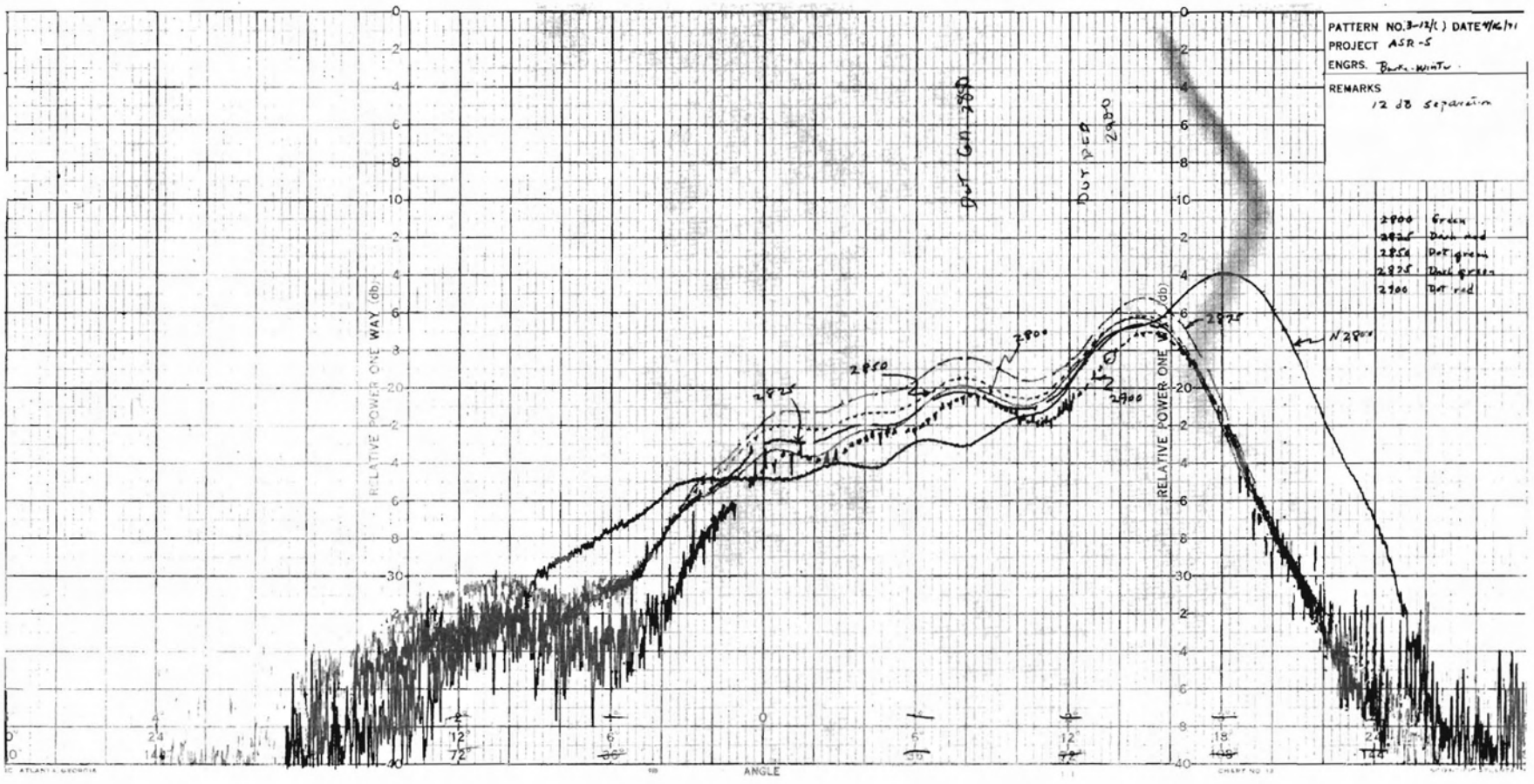

Figure 60. Second Feed Elevation Patterns from 2.8 GHz to 2.9 GHz

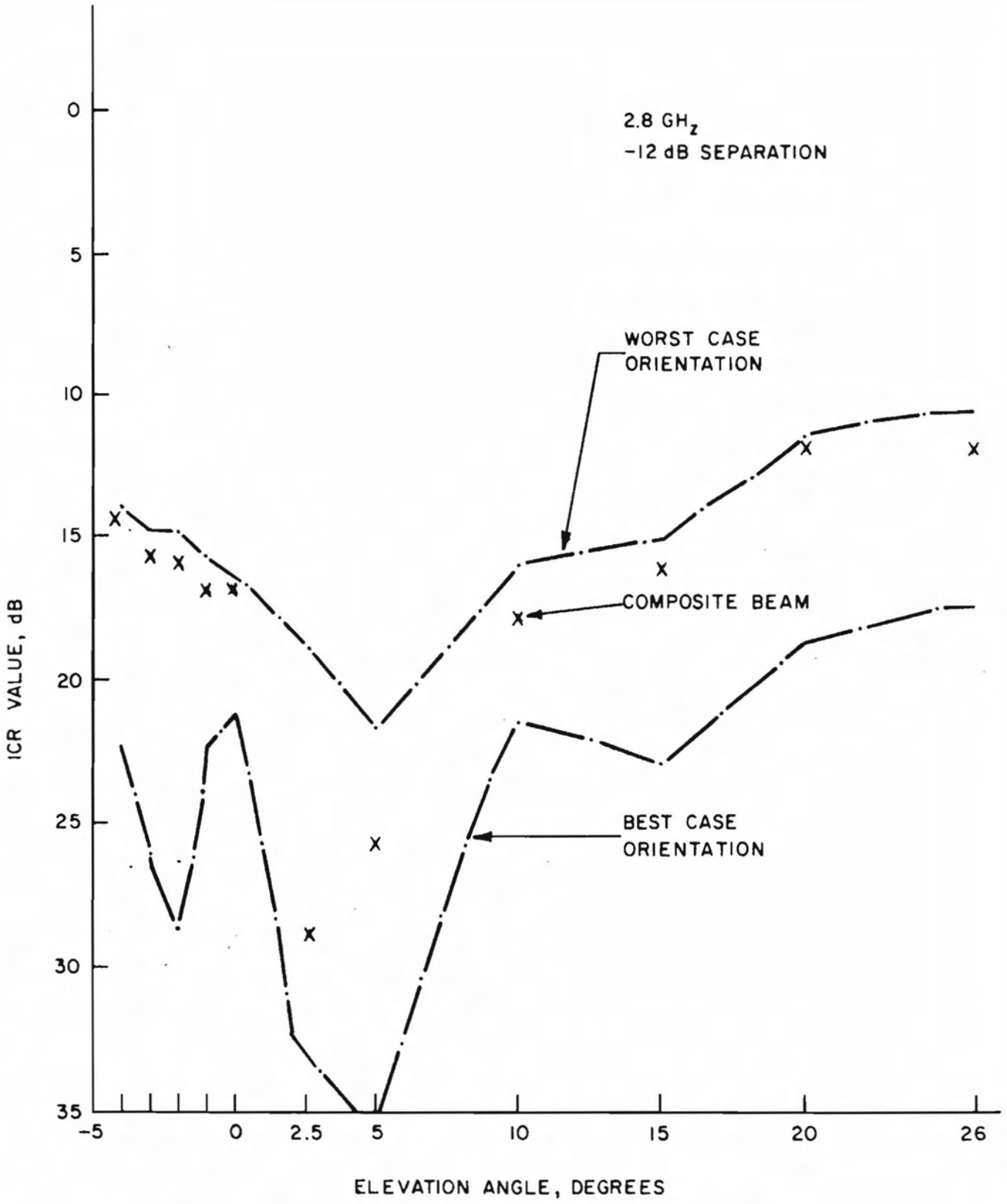

Figure 62. Azimuth Plane ICR Values (-12/2.8)

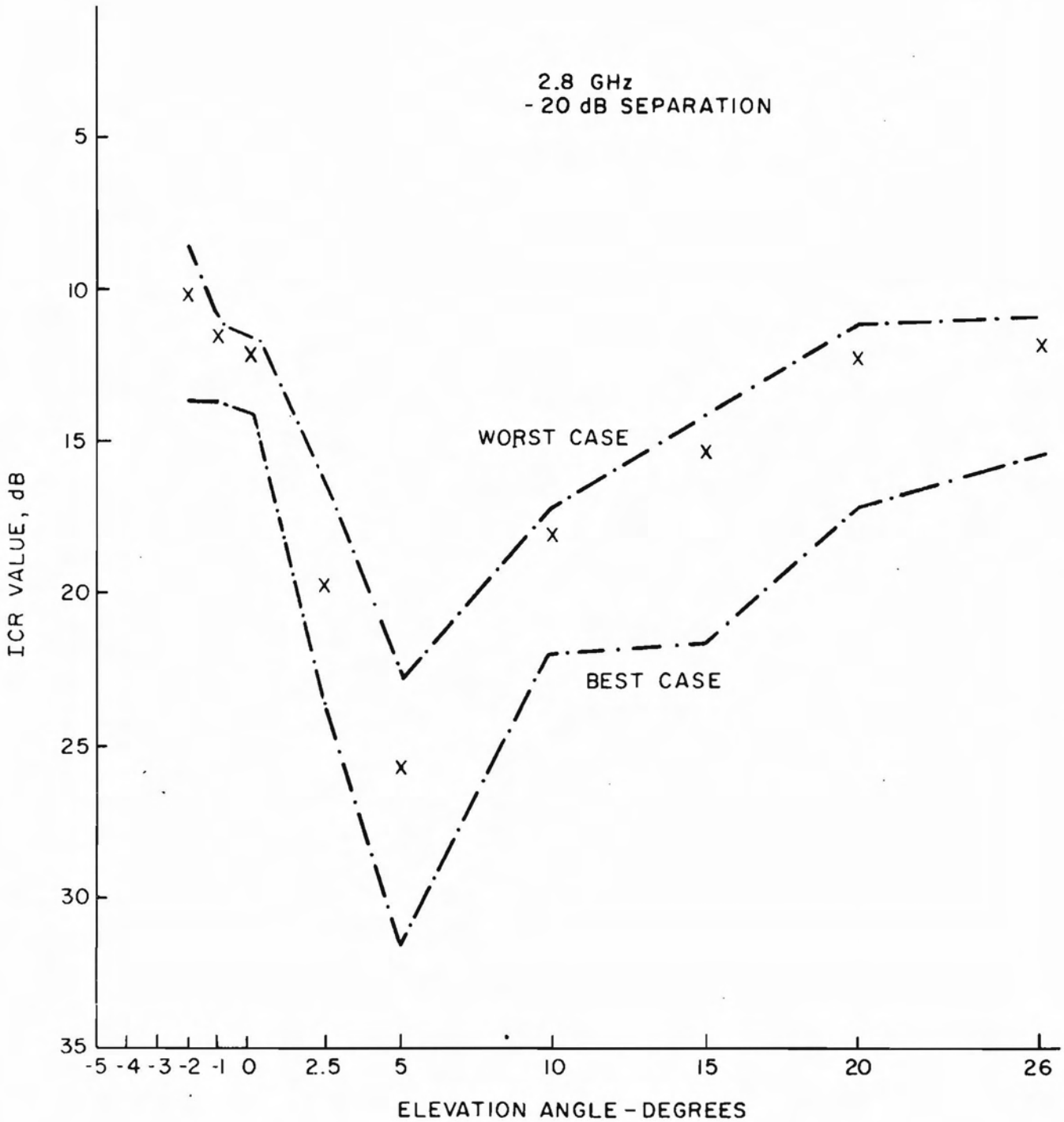

Figure 64. Azimuth Plane ICR Values (-20/2.8)

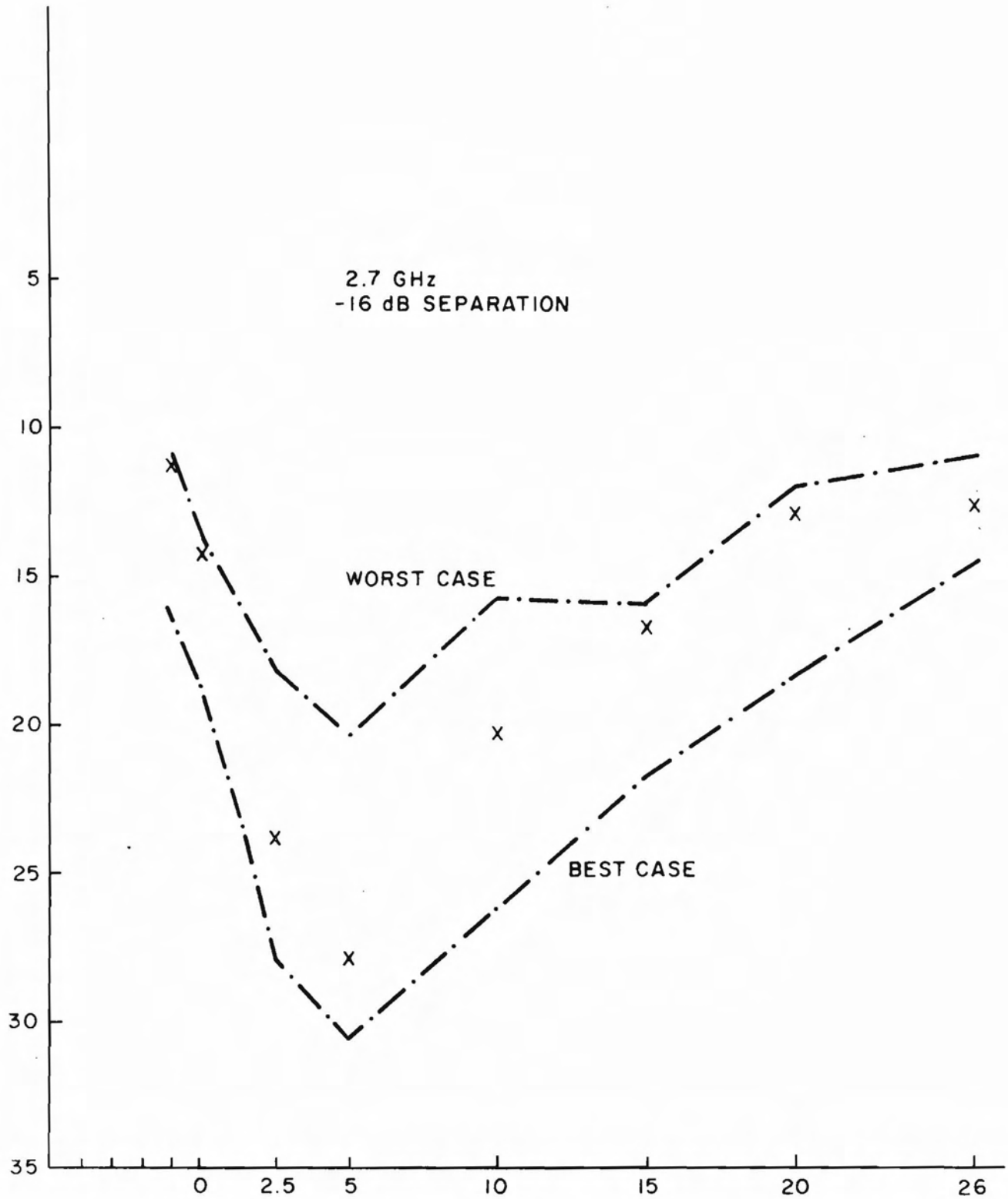

Figure 66. Azimuth Plane ICR Values (-16/2.7)

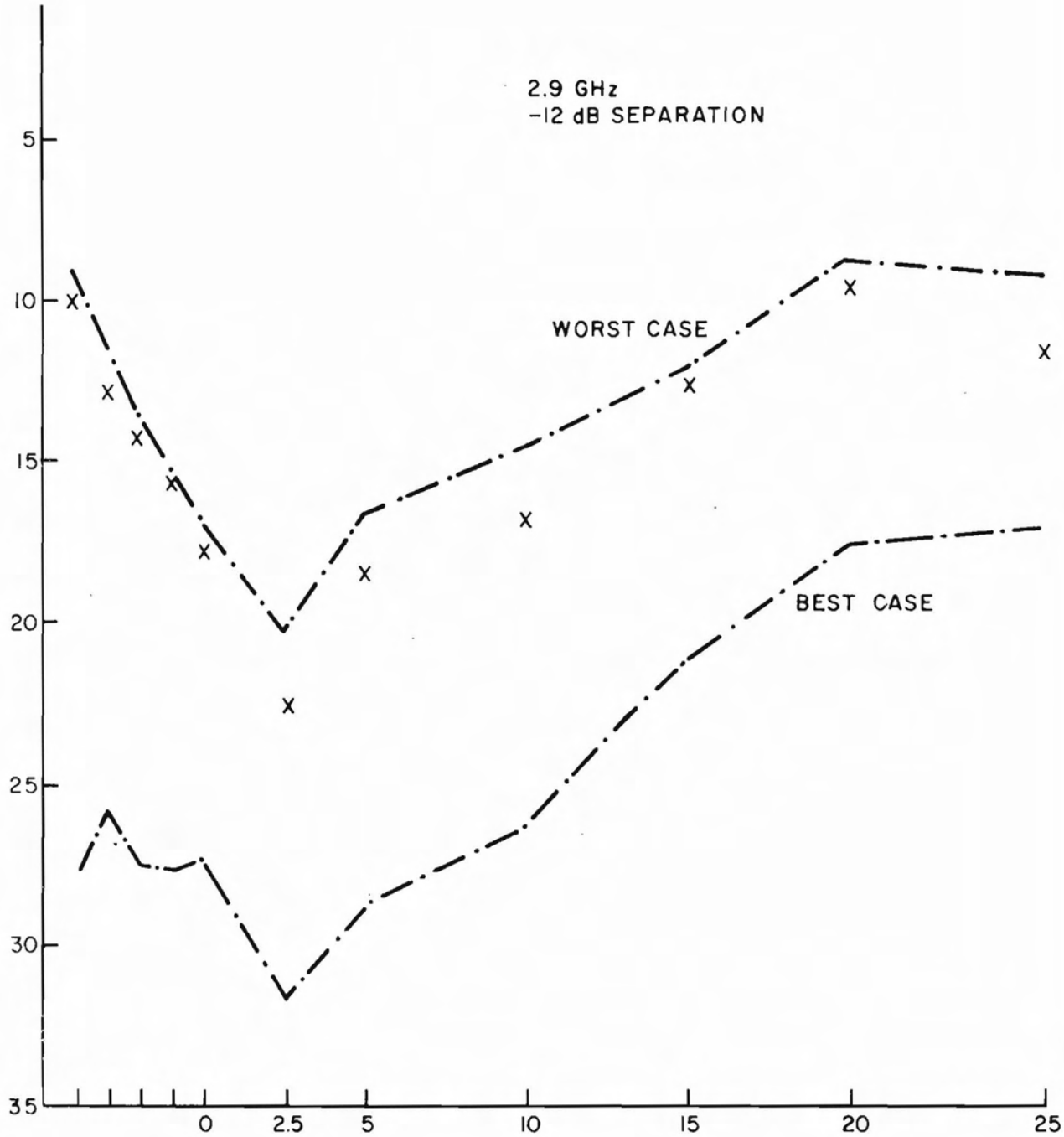

Figure 68. Azimuth Plane ICR Values (-12/2.9)

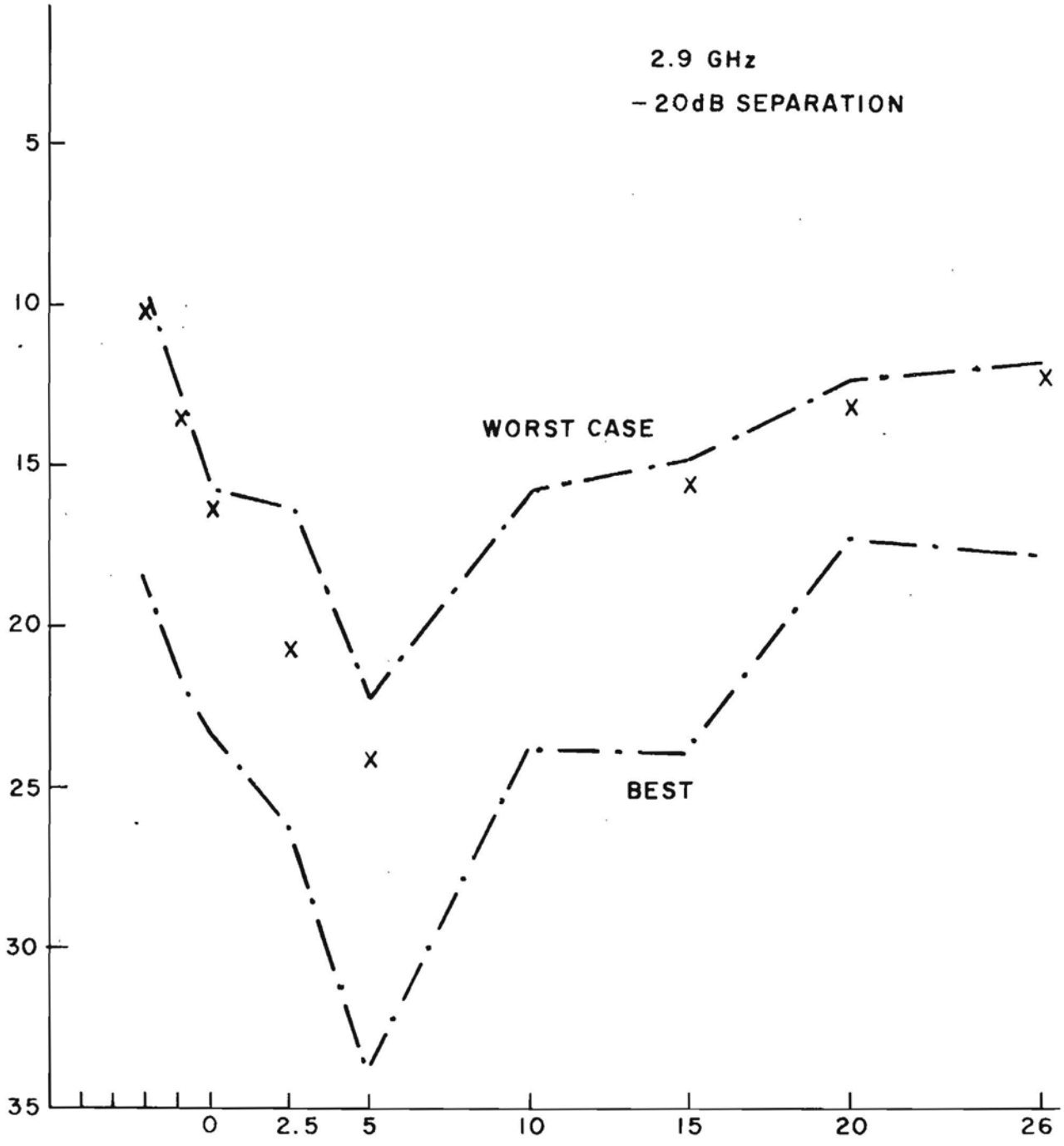

Figure 70. Azimuth Plane ICR Values (-20/2.9)

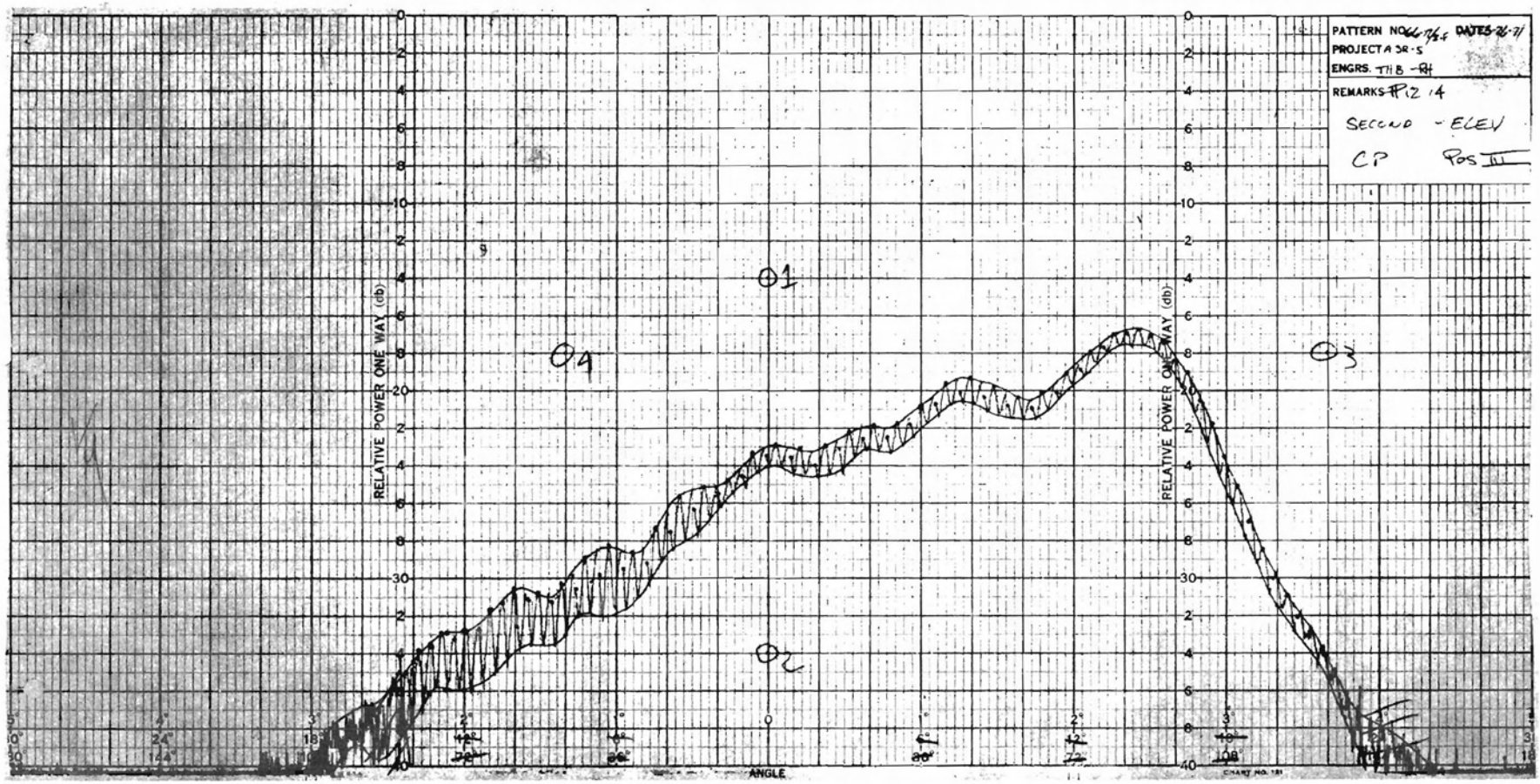

Figure 72. Second Feed Elevation Pattern for ICR-Calculation

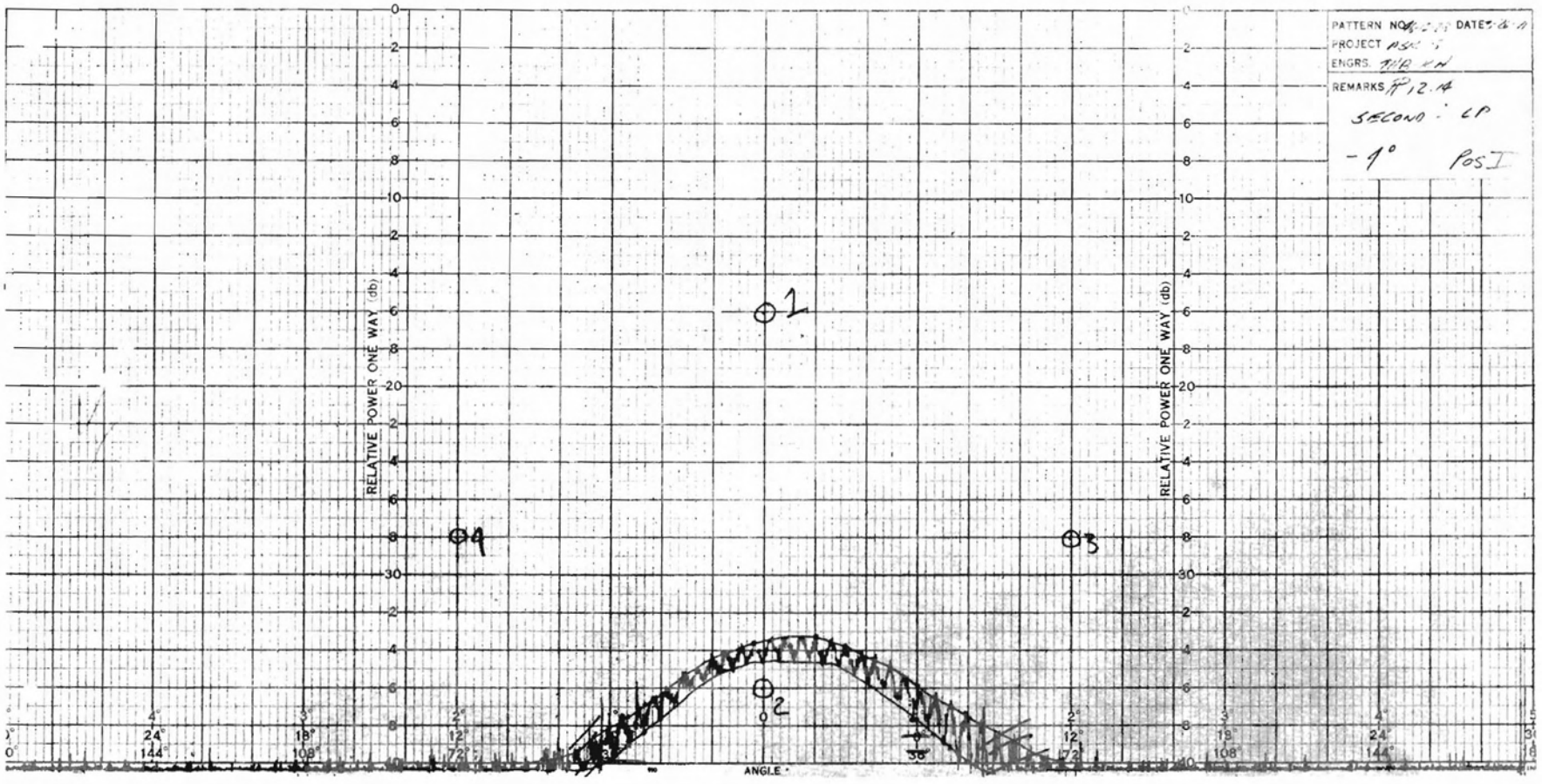

Figure 74. Second Feed Azimuth Cut at 4° for ICR-Calculation

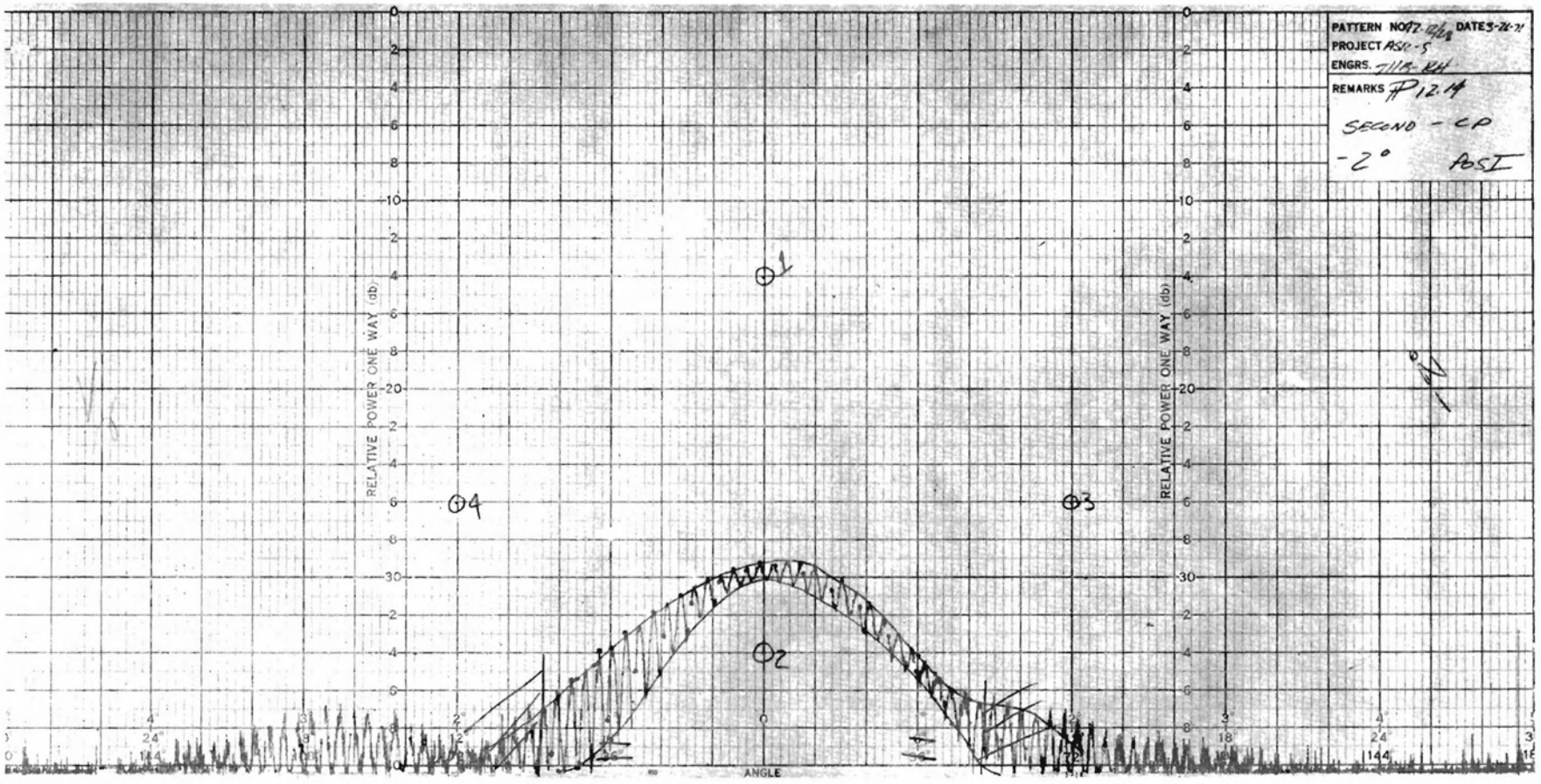

Figure 76. Second Feed Azimuth Cut at -2° for ICR-Calculation

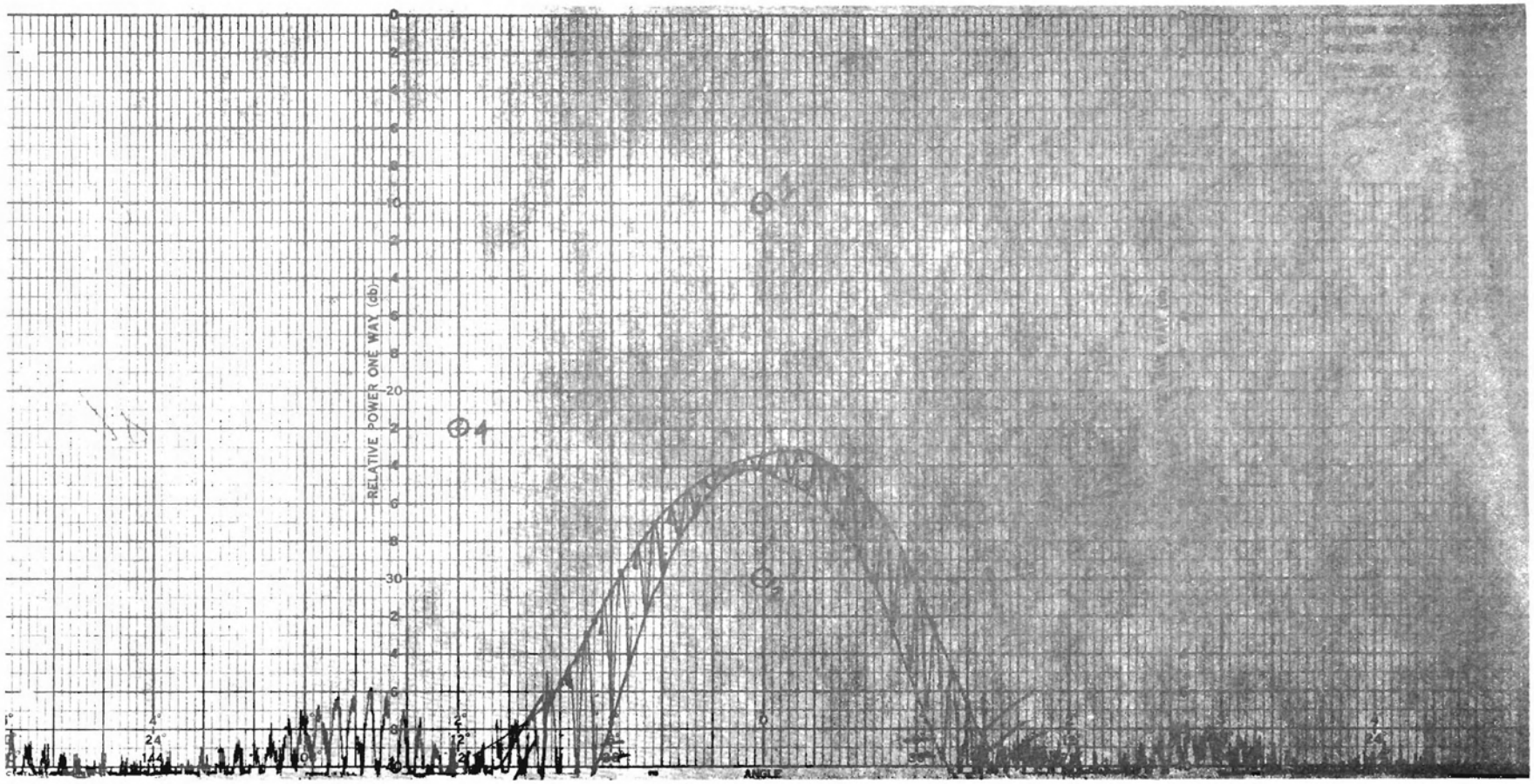

Figure 78. Second Feed Azimuth Cut at 0° for ICR-Calculation

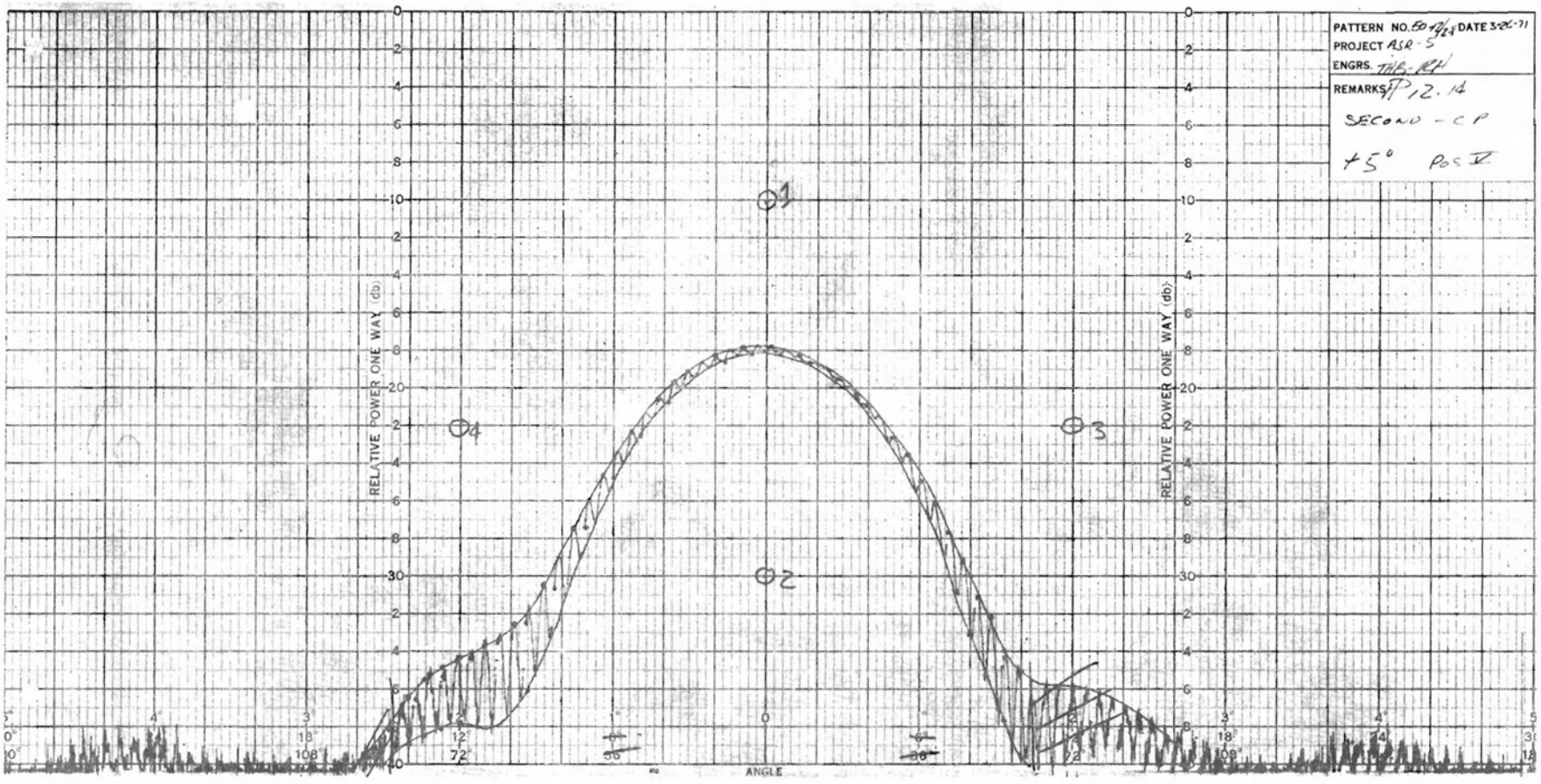

Figure 80 Second Feed Azimuth Cut at 5° for ICR-Calculation

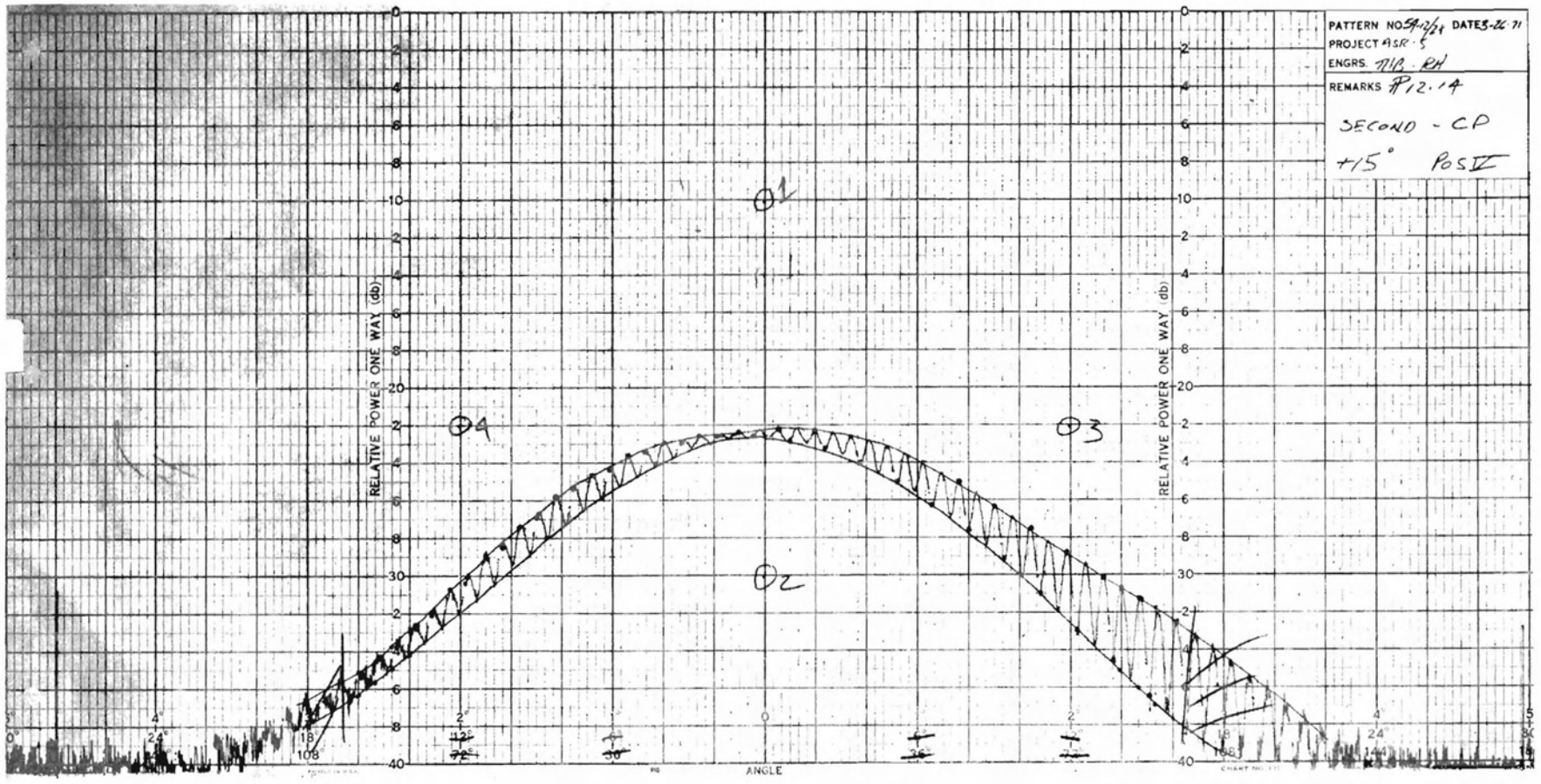

Figure 82. Second Feed Azimuth Cut at 15° for ICR-Calculation

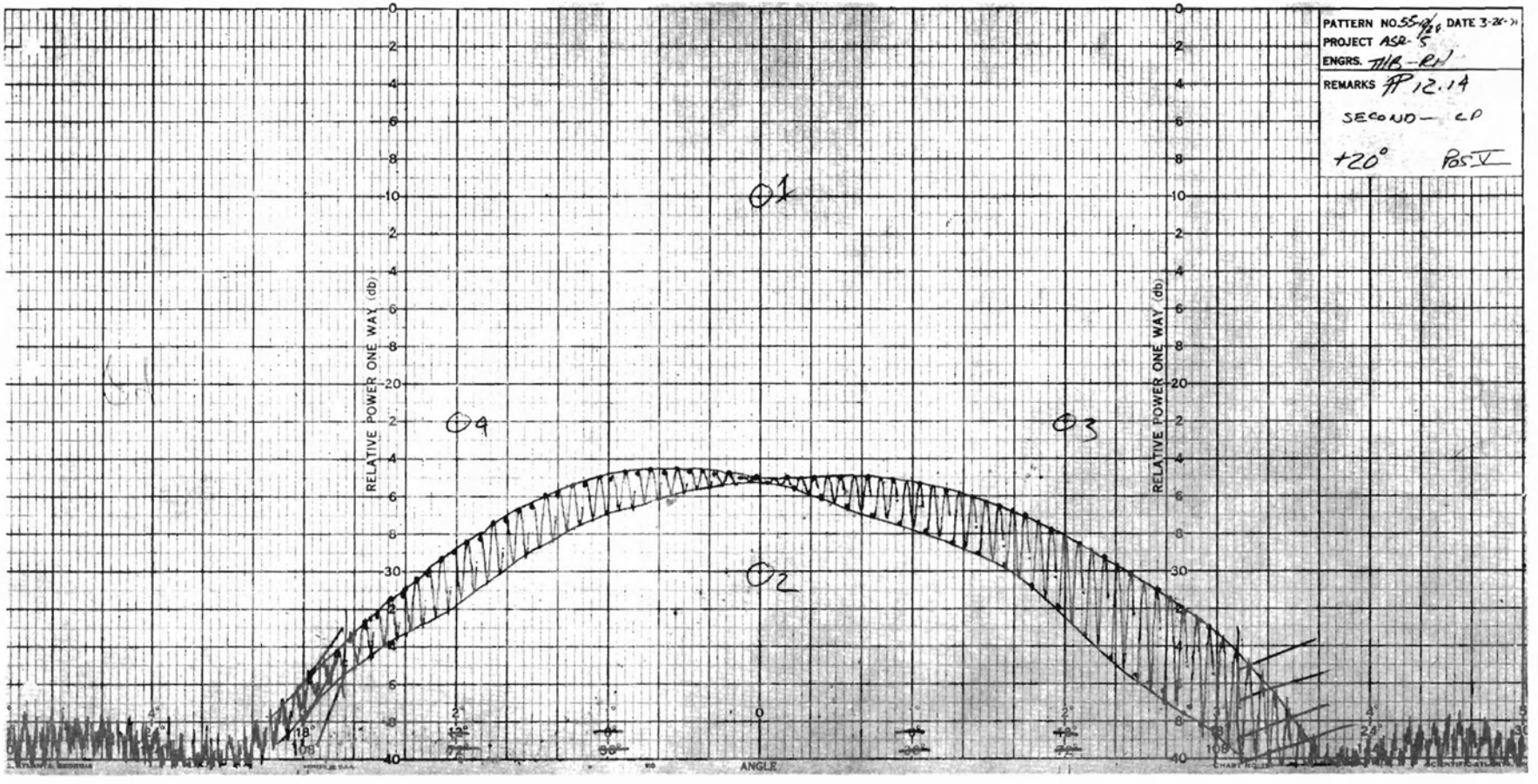

Figure 84. Second Feed Azimuth Cut at 20° for ICR-Calculation

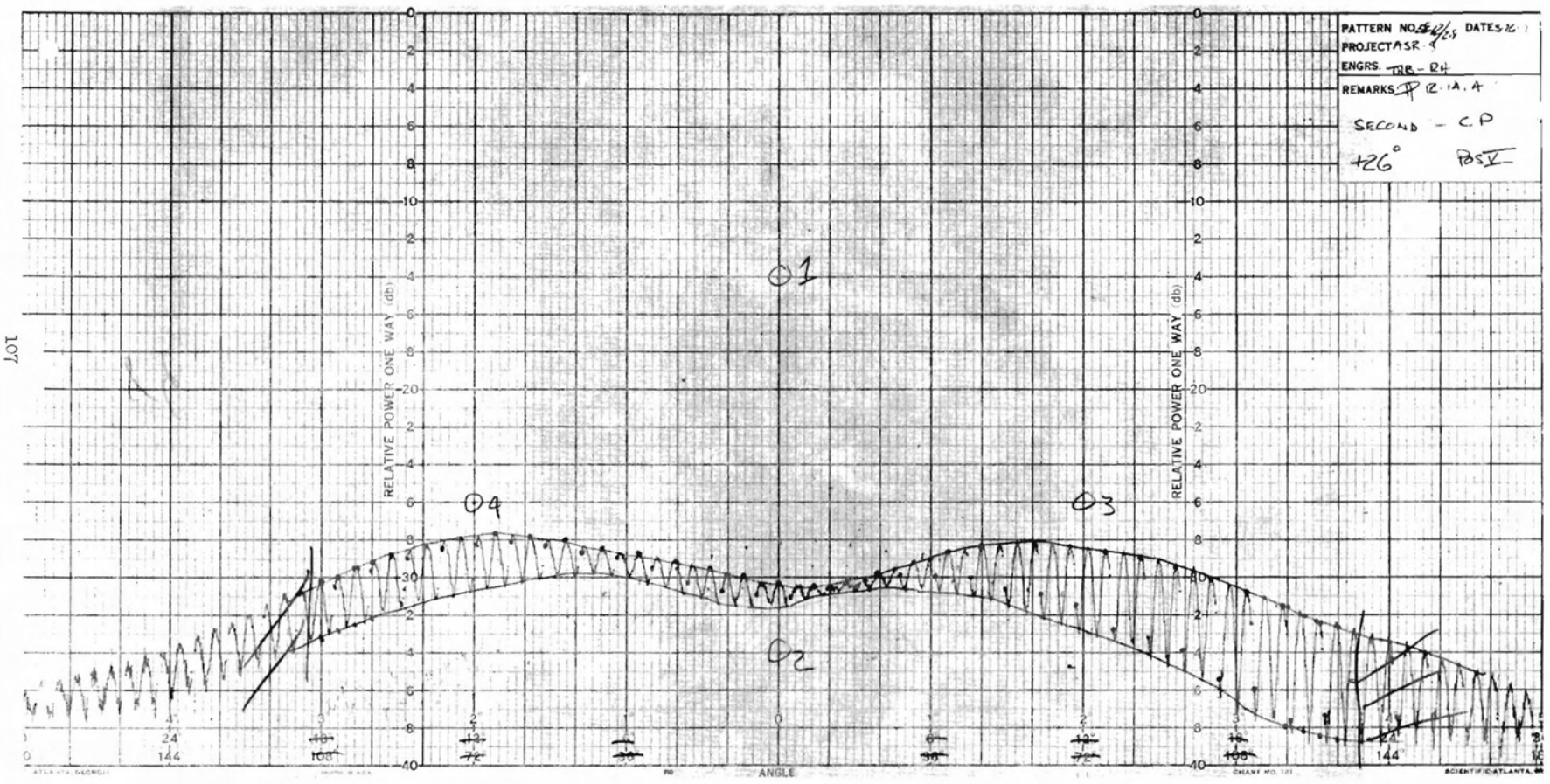

Figure 86. Second Feed Azimuth Cut at 26° for ICR-Calculation

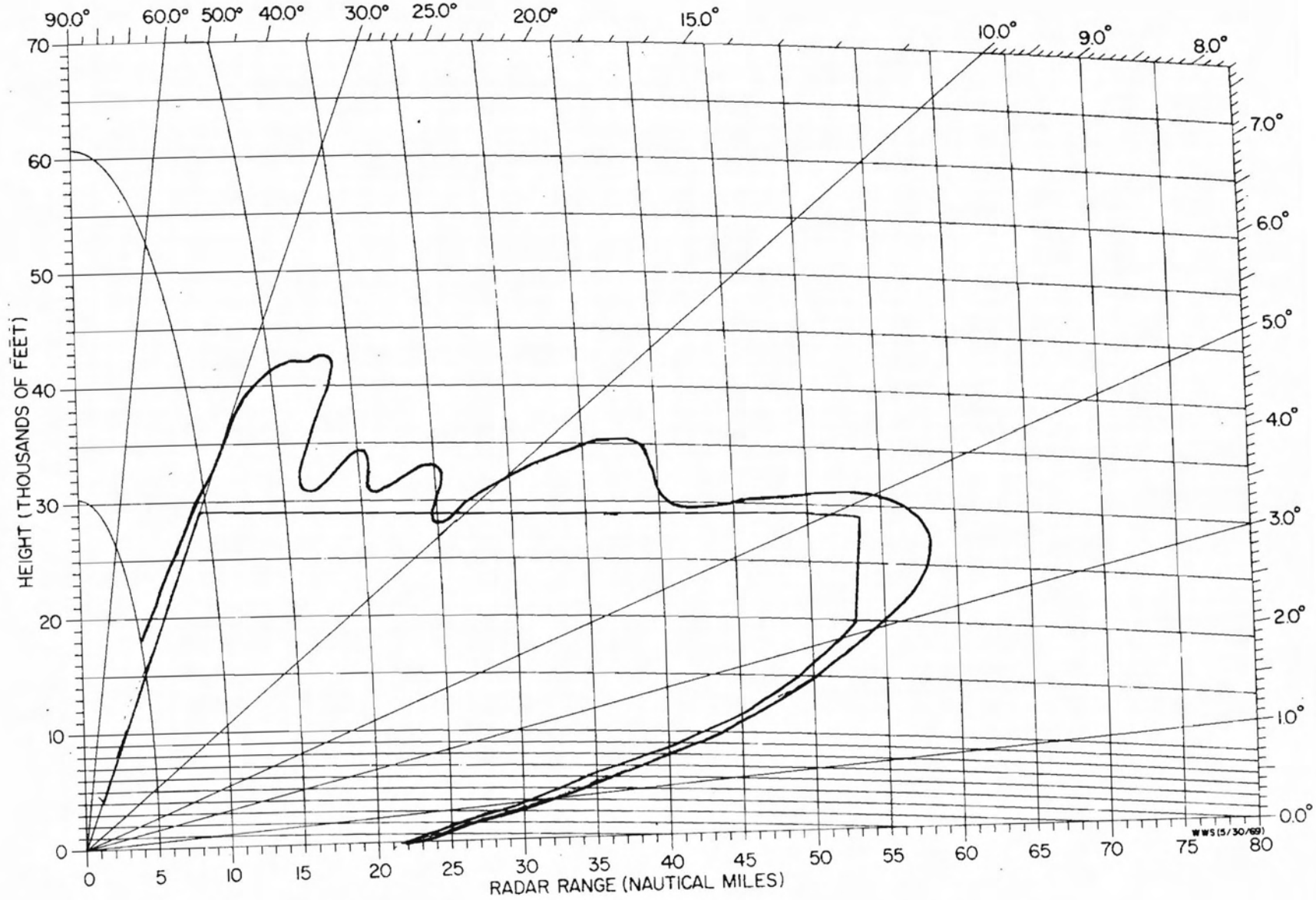

Figure 87. ASR Free-space Coverage for Unmodified Antenna

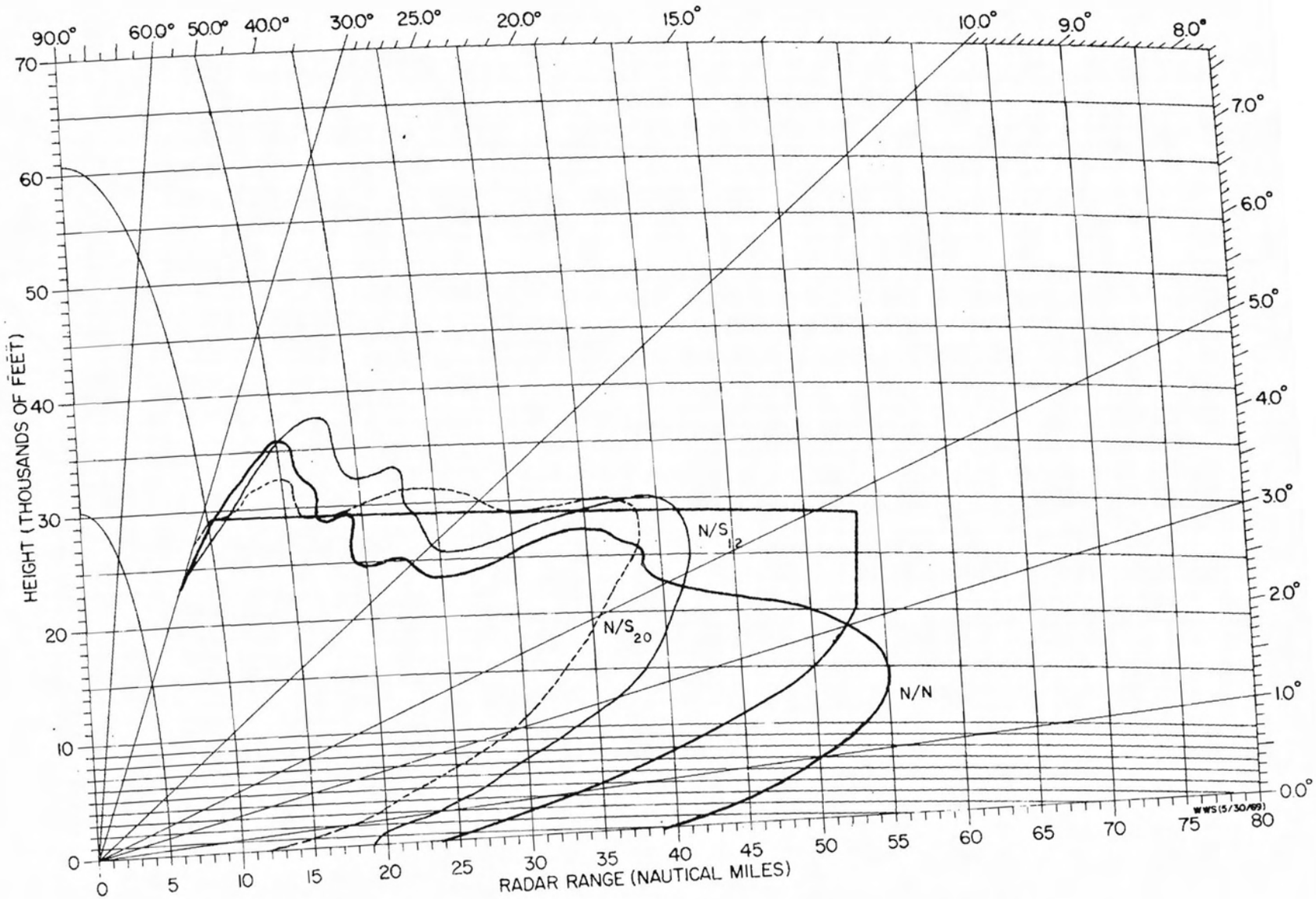

Figure 89. Two-way Coverage Plots for Modified Antenna

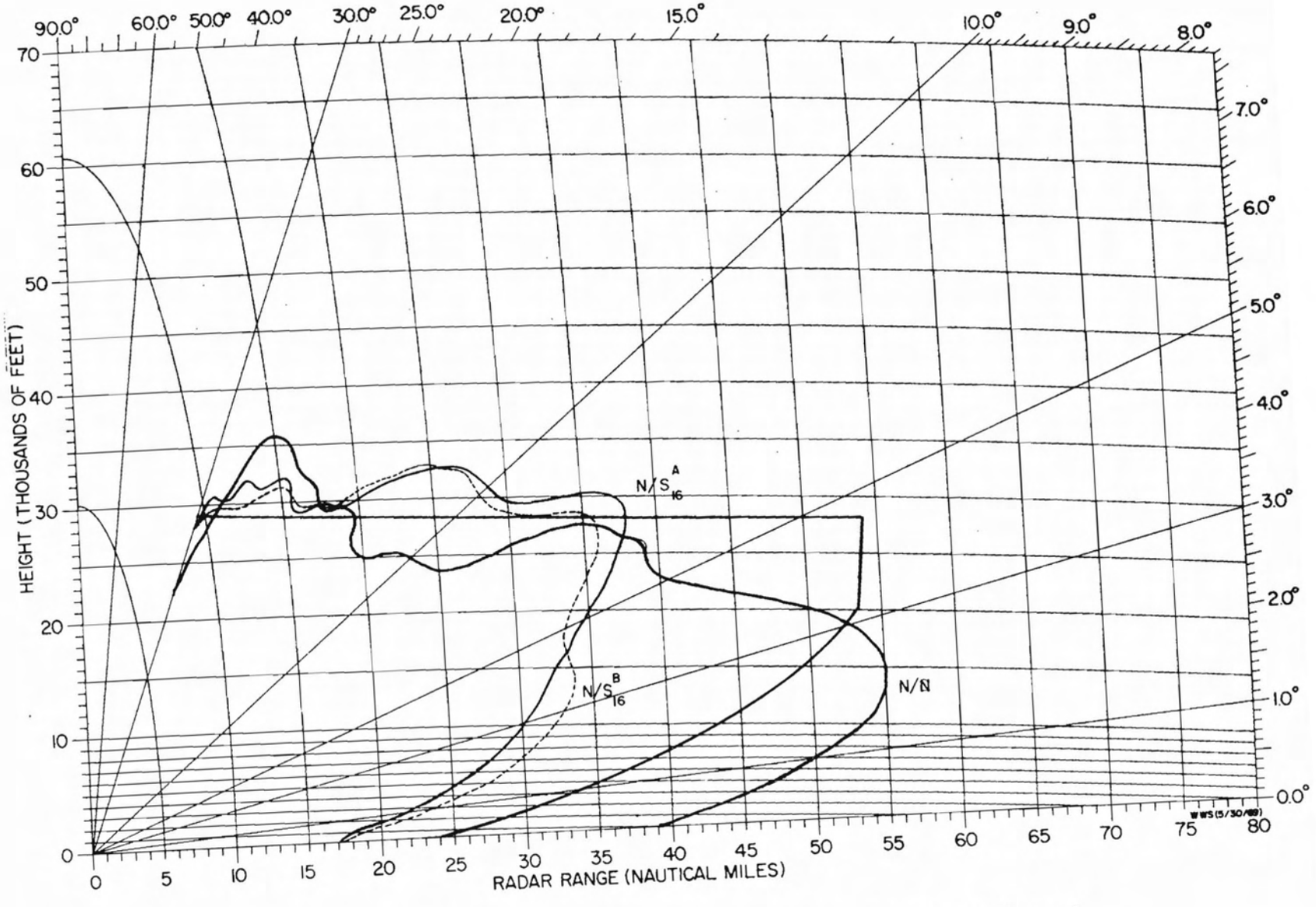

Figure 91. Variation in Two-way Coverage as Underside Slope Altered

CONCLUSIONS

It is concluded that:

1. The beam separation conditions of -12 dB, -16 dB, and -20 dB required in Paragraph 3.5 of FAA-ER-240-12 have been satisfied by an RF-combining, receive-only, network associated with a dual-feedhorn assembly for the ASR-5 antenna reflector.

2. The sidelobe levels, azimuth beamwidths, and elevation beamshapes of the second receive-only patterns are very similar to those characteristics of the unmodified ASR-5 antenna with the exception of moderate high angle beam broadening and increased cross-polarization level.*

3. Minimal degradation of the normal ASR-5 antenna pattern for both linear and circular polarization has occurred as a result of adding a second feedhorn, polarizer switch and new radome to the antenna geometry. However, the cross-polarization level has increased.*

4. The technique of employing an RF-combining network has proven that a single optimum position and tilt for the second feedhorn is permissible for all of the specified beam separation conditions.

5. Very good integrated cancellation ratios for the composite patterns of transmission on the normal beam and reception on the second RF-combined beam were obtained. The ICR of the composite patterns is as good as or better than that of either of the independent patterns.

6. The second feedhorn, its polarizer switch, and the RF-combining network, all of which have been implemented in breadboard model form for the Phase I experimental measurements, have been shown to be electrically consistent in performance.

7. It was demonstrated that calibration of phase and amplitude of the RF-combining network is feasible as an in-field adjustment.

8. Phase deviations up to ± 15°, which might result from changes in environmental conditions following calibration adjustment, do not significantly affect the beam separation, underside slope, or upper angle gain characteristics of the combined beam patterns.

9. A retrofit program to provide in-field modifications incorporating the two-beam technique in ASR-5 radar systems is feasible.

* Although the cross-polarization levels are higher in the modified antenna, the degradation is not regarded as important because good ICR values were obtained. See discussion on p. 60.